МИНИСТЕРСТВО НАУКИ И ВЫСШЕГО ОБРАЗОВАНИЯ РОССИЙСКОЙ ФЕДЕРАЦИИ

ФЕДЕРАЛЬНОЕ ГОСУДАРСТВЕННОЕ БЮДЖЕТНОЕ ОБРАЗОВАТЕЛЬНОЕ УЧРЕЖДЕНИЕ ВЫСШЕГО ОБРАЗОВАНИЯ

«НОВОСИБИРСКИЙ ГОСУДАРСТВЕННЫЙ ТЕХНИЧЕСКИЙ УНИВЕРСИТЕТ»

Кафедра материаловедения в машиностроении

Утверждаю

Зав. кафедрой ММ

_____ В. А. Батаев

«___» _____ 2021 г.

МАГИСТЕРСКАЯ ДИССЕРТАЦИЯ
по направлению высшего образования

22.04.01 Материаловедение и технологии материалов

Механико-технологический факультет

Витошкин Игорь Евгеньевич

Изучение структуры и свойств соединений разнородных материалов, полученных лазерной сваркой

Руководитель от НГТУ	**Руководитель от организации**	**Автор выпускной квалификационной работы**
Никулина А. А.	Маликов А.Г.	Витошкин И. Е.
к.т.н., доцент	к.т.н.	МТФ, Маг-961

Новосибирск 2021

МИНИСТЕРСТВО НАУКИ И ВЫСШЕГО ОБРАЗОВАНИЯ РОССИЙСКОЙ ФЕДЕРАЦИИ

ФЕДЕРАЛЬНОЕ ГОСУДАРСТВЕННОЕ БЮДЖЕТНОЕ ОБРАЗОВАТЕЛЬНОЕ УЧРЕЖДЕНИЕ ВЫСШЕГО ОБРАЗОВАНИЯ

«НОВОСИБИРСКИЙ ГОСУДАРСТВЕННЫЙ ТЕХНИЧЕСКИЙ УНИВЕРСИТЕТ»

Кафедра материаловедения в машиностроении

Утверждаю

Зав. кафедрой ММ

_____ В. Г. Буров

«___» _____ 20__ г.

ЗАДАНИЕ
НА МАГИСТЕРСКУЮ ДИССЕРТАЦИЮ

студенту *Витошкину Игорю Евгеньевичу*

факультета *Механико-технологического*

Направление подготовки *22.04.01 Материаловедение и технологии материалов*

Магистерская программа *«Высокоэнергетические технологии»*

Тема *Изучение структуры и свойств соединений разнородных материалов, полученных лазерной сваркой*

Цель работы: *определить процессы, возникающих при разнородной лазерной сварке титанового и алюминий-литиевого сплавов, и влияния на них смещения источника нагрева в сторону титановой пластины*

Задание согласовано и принято к исполнению.

Руководитель от НГТУ	**Руководитель от организации**	**Студент**
Никулина А. А.	Маликов А. Г.	Витошкин И. Е.
к.т.н., доцент	к.т.н., научный сотрудник	МТФ, Маг-961

Тема утверждена приказом по НГТУ № _____ от «____» _____ 201__г.

изменена приказом по НГТУ № _____ от «____» _____ 2021 г.

Диссертация сдана в ГЭК № _____, тема сверена с данными приказа

_____

(подпись секретаря государственной экзаменационной комиссии по защите ВКР, дата)

_____

(фамилия, имя, отчество секретаря государственной экзаменационной комиссии по защите ВКР)

ABSTRACT

Dissimilar welding is a prospective research field. Such techniques can allow to combine advantages of several materials in productive and easy automatized way. But as a rule, there are challenging problems related to brittle intermetallic compounds formation and thermal properties differences.

Ti/Al hybrid structures are of interest for such industry fields where structure mass has the same importance as its durability and strength. Such fields are aircraft and space industry. Despite the importance of such structures classical weld joints of Ti and Al alloys have low ductility due to intermetallic compounds formation. Together with significant differences in melting point, thermal conductivity and thermal expansion of these materials, it leads to low strength and cold cracks formation in these joints.

This work provides a study of processes which occur during dissimilar laser welding of Ti and Al-Li alloys. Both cases when the melts of the alloys interacted with each other and when melted Al interacted with solid Ti (welding-brazing) were considered. Such weld formation modes were achieved via laser beam focus displacement towards the Ti plates of several displacement values. To achieve the goal tensile tests, structural study and synchrotron radiation diffraction analysis were carried out.

The first chapter provides literature review on existing patents and scientific publications on dissimilar welding for Ti/Al and other metal couples. In this chapter it was concluded that the processes occurring during mixing of melts remain unexplored enough in Ti/Al welding. Based on this the purpose of this work was formylated as to determine the processes that occur during dissimilar laser welding of titanium and aluminum-lithium alloys

The second chapter describes the study procedures which were executed in this study. Also, this chapter contains the description of the experimental procedure.

The third chapter presents the research results and their analysis. It was found that the laser focus displacement positively influences strength of the joints increasing it from 76 MPa (when welded without the beam displacement) to 168

MPa (for the displacement of 1 mm). Structural study showed that insufficient displacement leads to thick (~800 μm) intermetallic layer formation which consist of α_2Ti_3Al, γTiAl and β_2Ti. Welding with sufficient beam displacement aloud to avoid the alloys melts interaction. Instead of this the joint formed via interaction between Al melt and solid Ti. In this case a thin (~2 μm) $TiAl_3$ intermetallic layer was formed. It is also important that in all cases melting and subsequent crystallization of Al alloy led to its softening in such zones. Because of this such joints cannot reach the base Al alloy strength even when intermetallic layer formation was suppressed.

The fourth chapter describes labor and environmental protection features in the laboratory at which this study was performed

The last chapter provides the economy calculations of present study. It was fount that this work took 56651.9 rubles to be performed.

This paper contains 73 pages, 35 pictures, 9 tables, 1 appendix and also it refers to 64 literature sources.

CONTENT

INTRODUCTION

Dissimilar welded joints are of increasing interest for modern structures [1,2], since this can allow combining the advantages of several materials, and the welding technology ensures the manufacturability of the manufacturing process of these structures. For example, hybrid structures Fe/Al [3] or Ti/Al [4], which combine the high strength of steel or titanium alloys and the low density of aluminum alloys.

Ti/Al joints are especially interesting for the aircraft industry, as both materials have low density and the resulting high specific strength, which is very important for aircraft structures. However, Ti/Al joining turned out to be challenging, since these materials have significant differences in physical (Table 1) and chemical properties. Differences in chemical properties lead to the fact that the welding process provokes the formation of various intermetallic compounds with a low ability to plastic deformation, which makes it impossible for the relaxation of residual stresses after welding.

Table 1 — Some important for welding physical properties of titanium and aluminum

	Pure Ti	**Pure Al**
Melting point, °C	1668	660
Thermal conductivity, W/(m·K)	21.9	237
Thermal expansion (at 25 °C), μm/(m·K)	8.6	23.1

The task of welding titanium and aluminum alloys is solved with some success using methods that exclude the intense interaction of the melts of these materials. These methods are welding-brazing with various laser [1,5–9] and tungsten inert gas (TIG) [10–12], brazing [13,14], diffusion welding [15], friction stir welding [16–19], explosion welding [20], welding with displacement of the heating source [21–28].

The main principle of materials science states that the properties of a material are determined by its structure and chemical composition [29], which obliges to carry out structural studies of these joints to explain their properties. Understanding the influence of the structure and the distribution of various phases in it (including intermetallic compounds) on the properties of the joints obtained is the key to understanding the principles of creating reliable dissimilar welded joints.

1 METHODS OF Al/Ti WELDING (Literature review)

1.1 Patents on dissimilar welding

Patent search has provided 10 patents on dissimilar welding techniques. Full list of them is presented in Appendix A.

CN102229018A [30] discloses an argon arc welding method suitable for self-connection of a TiAl-based alloy material. The plasticity of the welded TiAl-based alloy is improved by thermal treatment before welding, so that the welding property of the TiAl-based alloy is improved; and the thermal treatment temperature selected before welding is 1,310 to 1,350 DEG C. The method comprises the following steps of: preparing a Ti-Al-Nb series filling material, wherein the Ti-Al-Nb series filling material contains 40 to 50 percent of Al, 0 to 10 percent of Nb, 0 to 3 percent of V, 0 to 2 percent of Mo, 0 to 4 percent of Cr and the balance of Ti; preheating a welded part by adopting an induction coil at the temperature of between 500 and 800 DEG C, wherein the preheating and welding operations are finished in an argon filled box in order to avoid the problems of oxidation and hydrogen absorbing embrittlement of the TiAl-based alloy and the like; and after the welding is finished, performing annealing and stress removal treatment on the welded piece, wherein the annealing temperature is 900 DEG C. Compared with the methods of electron beam welding, laser welding and the like, the welding method provided by the invention is simple and convenient in operation, low in cost and convenient for popularization, can be used for repair welding of defects of castings or forgings of the TiAl-based alloy, and is suitable for efficient self connection of the TiAl-based alloy.

Patent US4486647A [31] describes following method of Ti/Al welding: aluminum is joined to titanium by welding using so much welding energy that the temperature on the titanium side of the alloying melt boundary remains below 2000° C., while titanium and aluminum do, however, melt at the joint interface. In a weldment thus obtained, the base material alloys and aluminum filler of which contain at maximum 10% titanium, there is in the vicinity of the interface between titanium and aluminum only a discontinuous β-phase, dispersed in the aluminum matrix.

CN102554456A [32] discloses a dissimilar metal diffusion welding method for a titanium-aluminum based alloy and titanium alloy (TC4) added amorphous interlayer. The method includes the steps: performing pre-welding heat treatment for a titanium-aluminum based alloy to be welded at the temperature of 1330-1360 DEG C and preserving heat for 10-40min; and placing a test piece to be welded in a protective sleeve, preventing a non-welding contact surface of the test piece from plastic deformation at a high temperature, clamping a nickel-based amorphous band between the titanium-aluminum based alloy and a titanium alloy, and performing diffusion welding at the temperature of 860-910 DEG C and at the pressure of 60-85MPa. The tensile strength of a joint obtained by the method is 350-400MPa at normal temperature and reaches 80%-90% of that of a titanium-aluminum based alloy base metal, and the tensile strength of the joint is 430-470MPa at the temperature of 400 DEG C and reaches 90%-98% of that of the titanium-aluminum based alloy base metal.

CN102896406A [33] provides a TIG (tungsten arc inert gas) welding method of a titanium alloy and pure aluminum plates. The method adopts a welding wire at specific ratio, an active agent is coated on the welding wire, argon tungsten-arc welding to titanium and the pure aluminum plates is performed, not only pre-alumetizing treatment related in a vacuum diffusion welding technology is avoided, but also welding cost in a vacuum environment or a laser condition is reduced. Filling material and pure aluminum plate parent metal are sufficiently molten and mixed during a welding process and then are solidified to form a welding line, and an obvious fusion area exists; a high-melting-point titanium alloy and a molten welding wire filling metal have mutual effect to form brazed connection, so that two metal liquid phase Ti and Al are prevented from being mixed, a large amount of fragile Ti-Al intermetallic compound is prevented from being produced, and simultaneously, the active agent on the surface of the welding wire has an effect of welding penetration increasing, so that the an artistic welding connector without cracks is formed through the welding line. The welding method has the advantages

that production efficiency is improved, a performance of the connector is improved, and the welding method is convenient to operate.

CN102229019B [34] belongs to the technical field of welding, and relates to an argon arc welding method suitable for a TiAl-based alloy and a titanium alloy material. The method comprises the following steps of:

1. selecting a titanium alloy welding wire of TA0-1 or TC4 or the same brand as a welded titanium alloy base material as a welding filling material;
2. performing pre-welding thermal treatment on the TiAl-based alloy to be welded, wherein the thermal treatment temperature is 1,310 to 1,350 DEG C;
3. preheating a test piece to be welded or a part to be welded in an argon filled box by adopting an induction coil, and measuring the temperature of the welded TiAl-based alloy at the position within 20 millimeters far from a seam, wherein the preheating temperature is between 500 and 800 DEG C;
4. performing argon tungsten-arc welding in the argon filled box;
5. performing annealing thermal treatment on the welded piece after welding, wherein the full stress removal annealing temperature of the welded titanium alloy is selected as the thermal treatment temperature. The room temperature tensile strength of an obtained joint is 400 to 490MPa, and achieves 80 to 95 percent of that of the TiAl base material.

US5844198A [35] provides the following: For an implantable medical devices, a system is provided for welding electrically conductive ribbon, typically stainless steel, to electrically conductive wire, typically platinum, the melting point of steel being substantially lower than that of platinum. An aperture is formed in the ribbon having an opening smaller than that of the wire. The ribbon is engaged with the wire such that the aperture is generally coextensive with the wire. Thereupon, a pulse laser beam is directed transversely of the ribbon through the aperture and onto the wire to simultaneously melt the wire and the ribbon and to create a homogeneous mix of the molten steel and platinum in the region surrounding the aperture. Thereafter, operation of the laser beam is discontinued to allow solidification and thereby achieve a welded connection between the ribbon and the wire.

CN106735948A [36] relates to the technical field of laser welding, more particularly, to a kind of method for laser welding and its device of copper aluminum dissimilar metal. A kind of method for laser welding of copper aluminum dissimilar metal, wherein, comprise the following steps: before welding, copper aluminum dissimilar metal to be welded is first carried out into slope treatment respectively, it is made it have certain slope; two pieces of copper aluminum dissimilar metals to be welded that slope treatment will have been carried out are placed on welding bench, laser beam is irradiated on the slope of one block of metal material to be welded, and laser beam can be made to reflex to another piece of metal slope to be welded; metal dust is spread between two blocks of metal materials to be welded; laser beam is irradiated to its surface, mobile laser beam carries out the laser welding of copper aluminum dissimilar metal. The present invention is easy to conventional laser equipment (Output wavelength is at 1.06 10.6 micron) The metal materials such as welding reflectivity copper, aluminum very high. Absorptivity of the laser beam in copper aluminum surface is improve by various methods, is conducive to laser welding copper aluminum dissimilar metal.

CN102764934A [37] discloses an aluminum steel dissimilar metal laser welding-brazing welding method and filled powder. A preset powder filling method is adopted. The method comprises the following steps of: configuring a joint to be in overlap joint and butting of different thicknesses, wherein the overlap joint length is 4-10mm in overlap joint; in butting, assembling the aluminum steel with the clearance-free bottom surface on the same level; striking a laser spot on an aluminum alloy in overlap joint and butting, wherein the distance from the laser spot to the edge of an aluminum plate is 0-0.5mm; coating powder so as to cover the gloss on the surface of the aluminum alloy, wherein the coating width is 2-4mm; and protecting by adopting an inert gas, wherein the protection mode is as follows: frontage protection is adopted for overlap joint, and simultaneous protection of frontage and back surface is adopted for butting. When optimized welding technology parameters are adopted, the aluminum alloy is melted and steel is not

melted, thereby forming welding-brazing welding overlap joint and butting connection.

US9174298B2 [38] declares that to provide a joining method for dissimilar metals which are magnesium alloy and steel and difficult to be metallurgically directly joined to each other while oxide film is present at a joining surface. In order to join magnesium alloy material 1 and steel plate 2 to each other, a galvanized steel plate to which Zn—Al—Mg alloy plating (a third material) is applied is used as the steel plate 2. When joining is made, ternary eutectic melting of Al—Mg—Zn is caused, so that it is discharged together with oxide film 1 f and impurities from the joining interface while Al—Mg intermetallic compound such as Al3Mg2 and Fe—Al intermetallic compound such as FeAl3 are formed, thereby joining the newly generated surfaces of the magnesium alloy material 1 and the steel plate 2 to each other through a compound layer 3 containing these intermetallic compounds.

An object of US20050230371A1 [39] (Figure 1) is to provide a laser roll joining process for dissimilar metals capable of improving the joining strength of a joint by increasing the amount of generation of ductile intermetallic compound and a laser roll joining equipment. A laser roll joining process for dissimilar metals for joining a first metal sheet 3 and a second metal sheet 4 of different materials held in non-contact state by after only the first metal sheet 3 is heated by laser irradiation, pressing a heated portion of the first metal sheet 3 against the second metal sheet 4 with a pressure welding roller 15 so that they are brought into a firm contact with each other and subjected to plastic deformation, wherein a joining portion between the first metal sheet 3 and the second metal sheet 4 is cooled.

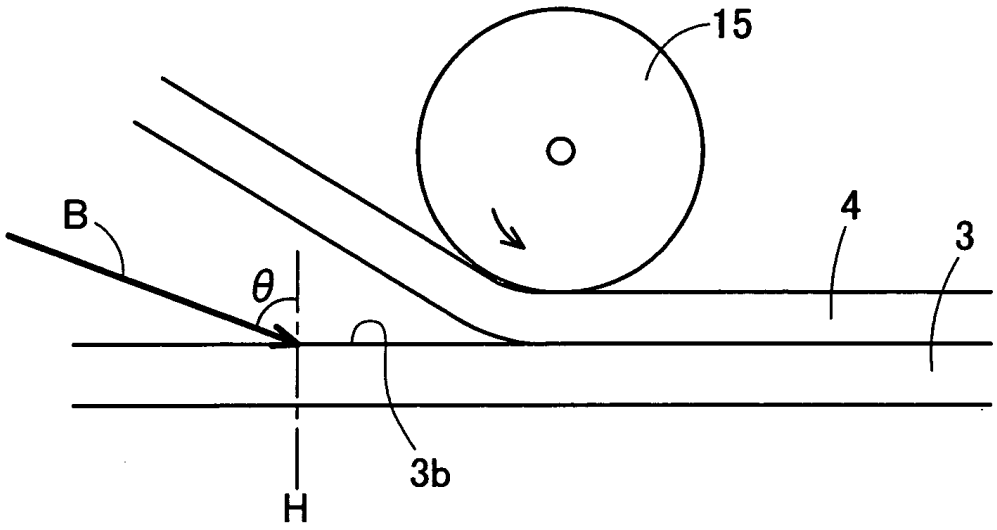

Figure 1 — A scheme for the US20050230371A1 patent

1.2 Publications on Ti/Al dissimilar welding

The main part of research in the field of welding titanium and aluminum falls on the so-called technique of welding-brazing, when a joint is obtained by contacting molten aluminum with solid titanium. For an example, Y. Chen, S. Chen and L. Li investigated how laser welding modes affect the strength and crack propagation in such joints. They found that both insufficiently long and too long interaction of the aluminum melt with titanium leads to the formation of a joint with low strength. The lamellae-shaped interface turned out to be the optimal structure [9].

Gas tungsten arc welding was used to create welded joints between titanium and aluminum alloys in [12]. In this work, the authors performed welding using an Al-Si filler wire and investigated the phase composition of the resulting joints. They claim that the interface consists of two layers – $Ti_7Al_5Si_{12}$ и $TiAl_3$.

I. Tomashchuk et. al. investigated the possibility of laser welding of titanium and aluminum alloys at high power and welding speed [40]. They found that high welding velocity reduces the thickness of the interfacial layer, increasing the strength of the joints. They also found that welding without offset leads to the formation of a thick intermetallic layer between the materials, due to which the strength was minimal (30-36% of base Al alloy vs 60% for the best welding mode).

Later I. Tomashchuk et. al. showed that the use of groove preparation and splitting the laser beam into two spots allow obtaining the desired structure of the joints, which had a positive effect on the properties of Ti / Al joints when welding-brazing Al-Si with solder [7].

In [6], the authors investigated the effect of welding parameters on the properties of joints between titanium and aluminum alloy, obtained by laser welding-brazing. They showed that by optimizing the parameters, it is possible to increase the strength of the joints up to 83% of the strength of the base aluminum alloy.

X. Chen et. al. carried out welding of titanium and aluminum alloys by oscillating laser radiation along the joint surface. By varying the parameters, they found that the strength of the joints can be increased up to 173 MPa [8].

The authors of [10] conducted a study of the influence of the TIG welding parameters on the structure and properties of the resulting joints. They showed that an increase in current increases the strength of the joints to a maximum of 235 MPa, after which it decreases. In this case, an increase in current also contributes to an increase in the thickness of the interlayer.

[11] introduces a new method for Ti/Al dissimilar welding called cold tungsten inert gas welding. The authors investigate interfacial microstructures of the joints and their influence on the properties of joints. In conclusion, they write that the interface consists of thin layers of $TiAl_3$ и $Ti_{3.3}Al$. The strength of the joints averaged 242 MPa.

Unlike most papers where titanium and aluminum are welded-brazed with wire, Z. Lei et. al. carried out this process using solder powder instead [1]. In their work, they investigated how the modes and the number of deposited layers affect the properties and structure of joints. It is shown in the work that an insufficient number of layers leads to insufficient wetting with the filler material. The optimal number of layers was from 5 to 7, while the strength of the joints was 240 MPa.

With an intention to reduce porosity and improve the wettability of titanium by X. Chen et. al. performed laser welding of titanium and aluminum alloys in

vacuum [5]. Analyzing the properties and structure of the joints obtained, they came to the conclusion that welding at 10 MPa leads to the best results, since the strength of the joints reaches a maximum of 181 MPa.

Z. Song et. al. performed laser welding-brazing of titanium and aluminum alloys without using filler material, but shifting the laser beam onto an aluminum plate [22]. After examining the structure and properties of the joints, they found that the thickness of the intermetallic layer strongly depends on the magnitude of the displacement, which affected the strength of the joints. The maximum strength was obtained with a displacement of 1 mm, which was 64% of the strength of the aluminum alloy.

Similarly, A. Nikulina et. al. obtained a laser welded joint of titanium alloy with aluminum in their work [27]. Having studied the structure of the joints, they came to the conclusion that welding-brazing leads to the formation of an intermetallic layer of TiAl3, the thickness of which must be reduced by varying the power, speed, or the amount of displacement of the laser beam on the aluminum plate.

In their work [28] G. Casalino et. al. achieved the formation of an Al/Ti weld joint by welding-brazing, shifting the laser radiation towards the titanium plate. In their work, they built a model close to the experiment, thanks to which they were able to find the optimal welding modes, in which the strength of the joints was obtained in ~ 90% of the strength of the aluminum alloy.

In the next work [21] G. Casalino et. al. investigated how the vertical and horizontal position of the focus affects the structure and properties of laser weld joints of titanium and aluminum alloys. They concluded that the thickness of the intermetallic layer can be controlled by varying these parameters, due to which it was possible to obtain joints with strength from 86 to 183 MPa and relative elongation from 1 to 7%.

There are also studies in which titanium and aluminum joints were made by brazing or solid-state welding. In one of such works [14], researchers used low-melting Al-Si-Cu-Ge solders with rare earth additions to create a brazed joint

between alloys. Their studies have shown that the addition of rare earth elements contribute to the refinement of aluminum grains in the solder and change the morphology of the Al2Cu phase from acicular to block, which also improves the structure of the solder.

X. Chen et. al. produced ultrasonic-assisted brazing of Al-Ti alloys [13]. To avoid cracking caused by a large difference in the thermal expansion of the alloys, the researchers used a solder with a wide gap between solidus and liquidus, which allowed the process to be carried out at lower temperatures. The use of such a solder made it possible to exclude the formation of cold cracks and to increase the shear strength from 43 to 76 MPa.

In [15] Y. Wei et. al. investigated the growth of an intermetallic layer between plates of pure Ti and Al upon heating. After examining the structure and shear strength, they concluded that the only phase formed under such conditions is TiAl3. Moreover, an increase in the thickness of this layer had a positive effect on the shear strength of such a joint.

Y. Mahmood et. al. joined titanium and aluminum alloys via explosion welding [20]. Structural study and mechanical tests have shown that explosion welding allows to obtain a high-quality joint despite the formation of various intermetallic compounds in the contact zone. Heat treatment of such compounds led to a decrease in their strength due to the growth of intermetallic structures.

C. Zhang et. al. investigated the distribution of alloying elements in the joints between titanium and aluminum alloys obtained by ultrasonic welding [41]. High-resolution STEM-EDS analysis showed that elements such as Si, Mg and O are concentrated in the interphase layer, while Cu and V are evenly distributed.

The authors of [19] obtained joints between titanium and aluminum alloys by friction stir welding in various welding modes. They found that both too high and too low a rotation speed resulted in poor bond strength, while a probe speed of 750 rpm produced a bond strength of 215 MPa, which is 68% of the strength of the base aluminum alloy.

J. Choi et. al. conducted a study of the influence of friction stir welding modes on the properties and structure of joints between pure Ti and Al [16], however, in addition to the previous work, the authors investigated the effect of probe displacement on the density of titanium fragments in the welding zone. They found that greater displacement on the titanium plate results in more titanium fragments in the weld zone. This was also influenced by the welding speed, but the offset played a decisive role in this.

The authors of [17,18] assumed that the presence of niobium [17] and zinc [18] foils between titanium and aluminum plates can increase the plasticity of intermetallic compounds formed during friction stir welding. Having studied the structure and properties of the obtained compounds, they found that the introduction of both niobium and zinc foils into the compound limits the formation of the brittle TiAl3 phase, due to which the compounds acquired greater plasticity.

1.3 Conclusion

As noted above, in most works, the authors try to avoid the interaction of titanium and aluminum melts in order to prevent the formation of brittle intermetallic compounds, thus performing brazing welding. This process is well understood. However, the processes occurring during mixing of melts remain unexplored enough. Although such joints appear less attractive due to their high brittleness, a lower chemical gradient along the cross-section can allow a decrease in the diffusion rate upon heating and, therefore, allow heat treatment and use at elevated temperatures of such compounds. Also, such joints are easier to design, since they do not groove preparation and filler material. Understanding the processes involved in the formation of such joints can help find effective ways to improve their properties.

In most works, the authors use alloys of the Al-Mg or Al-Mg-Si system. However, recently, aluminum-lithium alloys have been introduced as a replacement for these alloys in the aviation industry, which makes the study of the weldability of such alloys urgent.

Laser beam displacement has been shown to be a simple and effective method for controlling the processes occurring during laser welding of dissimilar materials.

1.4 Purpose and tasks of this work

Thus, the purpose of this work is to determine the processes that occur during dissimilar laser welding of titanium and aluminum-lithium alloys, and the effect on them of the displacement of laser radiation towards the titanium plate.

To do this the following experiments and study were performed:

- Laser welding of Ti and Al-Li alloys with different horizontal displacement towards Ti plate;
- Scanning electron microscopy of the obtained joints;
- Synchrotron radiation diffraction analysis (SRDA);
- Tensile tests.

2 MATERIALS AND RESEARCH METHODS

2.1 Materials

Titanium alloy VT-20 and aluminum alloy V-1461 in the form of sheets 2 mm thick and 100x50 mm in size were chosen for the experiments.

Alloy VT-20 is a pseudo-α alloy, which means the presence, in addition to the α-phase, of a small (about 1 vol.%) amount of β-phase in the structure of the material, which is provided by alloying with β-stabilizing elements (in this case, Mo and V) [42].

B-1461 is a high-strength heat-hardenable aluminum alloy of the Al-Cu-Li system. The main hardening effect is achieved by precipitating regions of an ordered solid solution (δ'Al3Li) and Al_xCuLi_y particles as a result of quenching and subsequent artificial aging [43].

Chemical composition of the chosen alloys is presented in Table 2 and Table 3.

Table 2 — Chemical composition of the VT-20 titanium alloy (according to GOST 19807-97 [44])

Ti, wt. %	**Fe, wt. %**	**C, wt. %**	**Si, wt. %**	**Mo, wt. %**	**V, wt. %**	**N, wt. %**	**Al, wt. %**	**Zr, wt. %**	**O, wt. %**	**H, wt. %**
balance	< 0.25	< 0.1	< 0.15	0.5-2	0.8-2.5	<0.05	5.5-7	1.5-2.5	<0.15	<0.015

Table 3 — Chemical composition of the V-1461 aluminum alloy

Al, wt. %	**Cu, wt. %**	**Mg, wt. %**	**Li, wt. %**	**Zn, wt. %**	**Zr, wt. %**	**Sc, wt. %**	**Mn, wt. %**	**Ti, wt. %**
balance	2.5 - 2.95	0.05	1.5 - 1.9	0.2 - 0.8	0.26	0.28	0.04	0.07

2.2 Experiment procedure

To remove oxide films, the surfaces close to the welding zone were ground and then etched with a saturated aqueous solution of NaOH.

The welding process was carried out with CO_2 laser with wave length of 10.6 μm at Institute of Theoretical and Applied Mechanics (ITAM SR RAS) on the automated laser technological complex "Sibir-4". The beam was focused using a ZnSe lens with a focal length of 254 mm. The spot size in focus was 200 μm. Welding was carried out at a radiation power of 1.2 kW at a speed of 1 m / min and a beam displacement of 0, 0.5 and 1 mm towards the titanium plate (Figure 2). The focus was 3 mm below the surface of the plates. A shielding gas (a mixture of argon and helium) was used to protect the weld from oxidation.

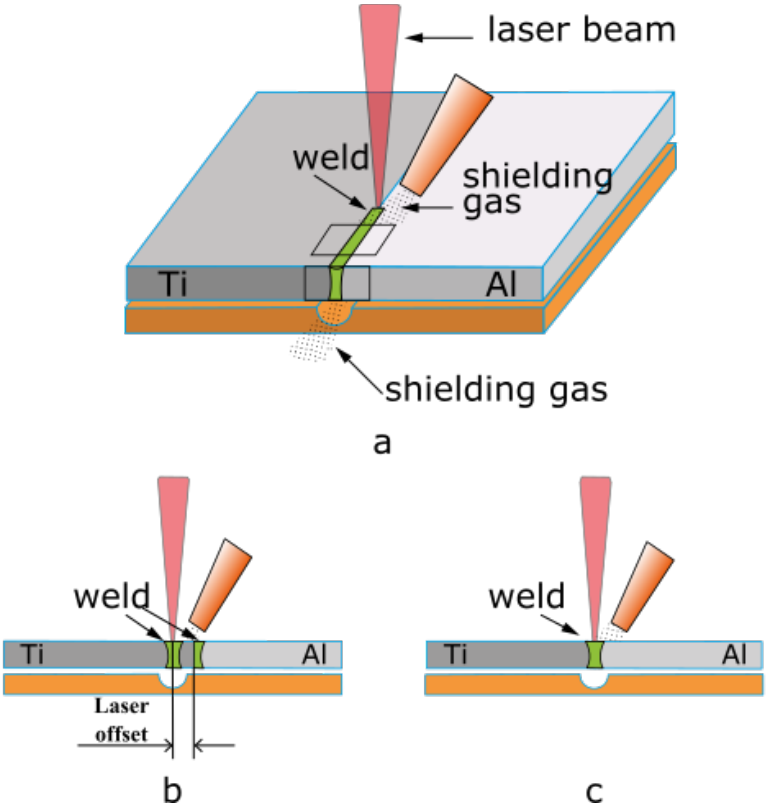

Figure 2 — The welding process scheme: a – shielding gas ventilation scheme, b – welding with offset scheme, c – welding with no offset scheme

2.3 Analysis procedure

As a part of the analysis procedure tensile tests, scanning electron microscopy (SEM) and synchrotron radiation diffraction analysis (SRDA) were used.

The tensile tests were conducted at Institute of Hydrodynamics SB RAS with tensile machine Zwick Roell. The samples had rectangle cross-sections with sizes of 2x10 mm. The length of the samples was 100 mm.

Scanning electron microscopy was carried out with EVO30 XVP microscope at ITAM SB RAS.

Filming of the diffraction pattern of the welded joints was carried out at the Institute of Nuclear Physics SB RAS at the VEPP-4 station. The beam had a rectangular section with dimensions of 400x100 μm. The process was carried out in sections along the entire joint, from the base material of one plate to the another one. The radiation wavelength was 0.3685 Å. The diffraction was recorded using a fluorescent screen located behind the sample (Figure 3, a). The obtained images (Figure 3, b) were integrated along circles into spectra (only a ¼ of the rings were used Figure 3, c)

SEM allowed to determine morphology and approximate chemical composition of the components which appear in the structure of the joints. Together with SRDA it was possible to identify the phases placement and morphology.

Tensile tests showed how the structure of the joints influences their strength.

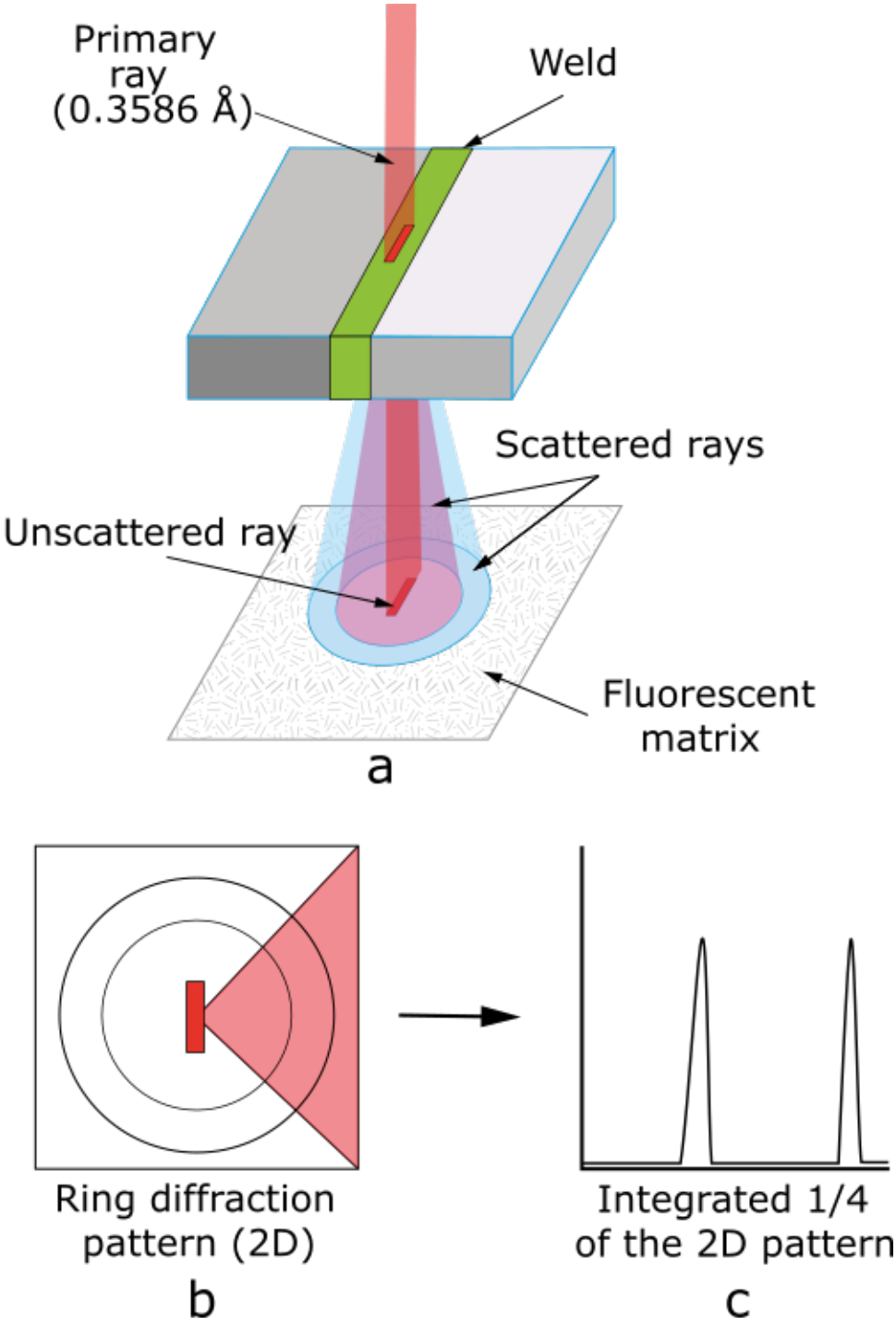

Figure 3 — Scheme of the synchrotron radiation diffraction analysis: a – the process scheme, b – the obtained diffraction image scheme, c – the obtained spectrum scheme

3 RESEARCH SECTION

3.1 Scanning electron microscopy

SEM study was performed at 3 joints of different welding modes: 0, 0.5 and 1 mm laser beam displacement towards Ti plate.

3.1.1 Welding without offset

Welding without beam offset resulted in intense mixing of the base materials, which led to large mixed zone (MZ) appearance at the center of the joint (Figure 4). A part of the aluminum alloy melt avoided such intensive mixing resulting in Al fusion zone (AL FZ) creation.

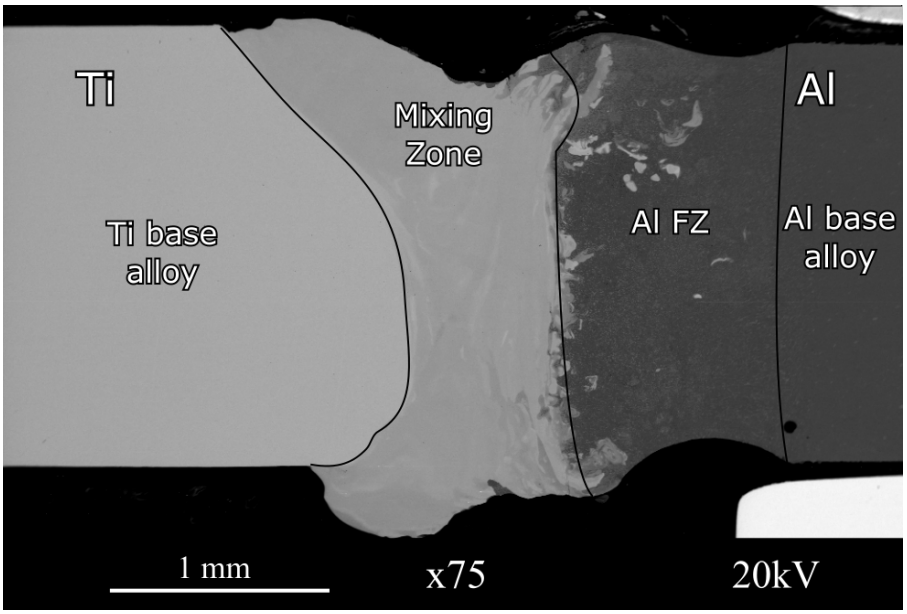

Figure 4 — The main view of the welded without offset joint structure (Back scattered electrons mode)

The base Al alloy (Figure 5, Table 4) contains Cu-rich precipitates with zise of less than 1 μm (spots 4 and 6). Also, it is extremely rare to find larger particles with a size of 6-8 μm (points 1 and 2).

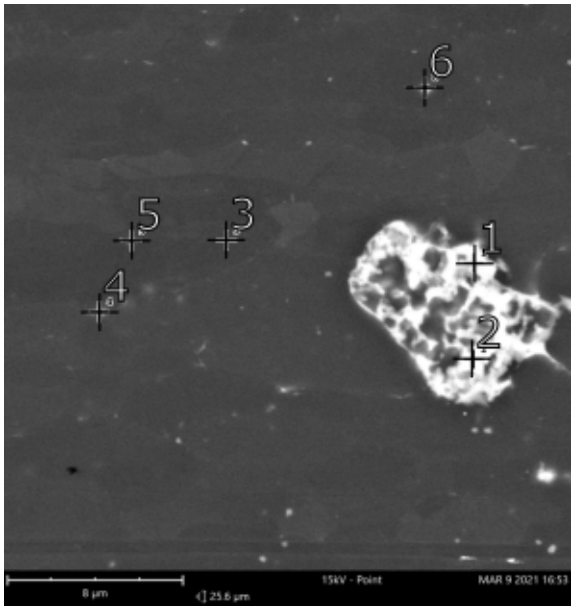

Figure 5 — The base Al-alloy structure

Table 4 — Chemical composition in the spots 1-6 (Figure 5)

Spot	Al, at.%	Cu, at.%
1	87.29	12.71
2	81.08	18.92
3	98.99	1.01
4	97.59	2.41
5	98.67	1.33
6	96.07	3.28

Near the Al FZ it can be seen that the Cu-rich phases are concentrated at the boundaries of the Al grains (Figure 6). Such phenomenon is a consequence of a heating above solvus temperature for these phases. Also, the shape of the Al grains is changed from elongated to equiaxed one, which is an effect of a heating plastically deformed metal alloy.

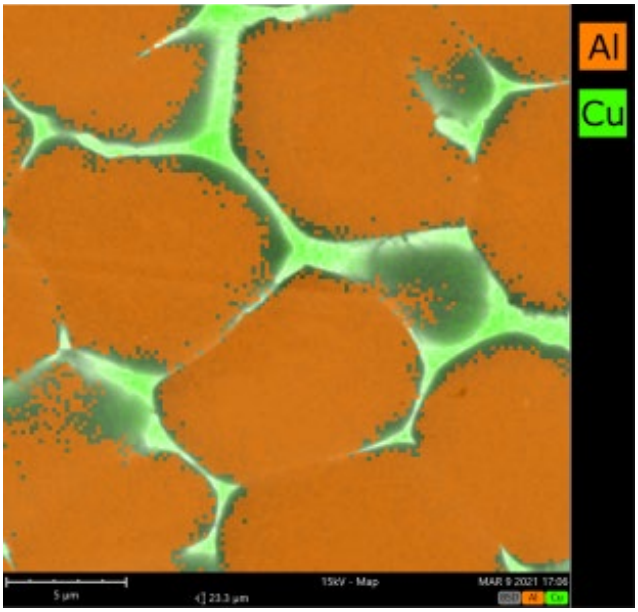

Figure 6 — The structure of the heat affected zone in the Al-alloy structure (Composition map)

Al FZ (Figure 7) contains the same net-like Cu-rich structure as the heat affected zone but also there are needle-like structure, which contain some amount of Ti. These structures are placed independently of the Al grains which means that the Ti-rich particles were the first phase which crystallized from the melt, after which Al grains were formed around the needle-like particles. Crossing the solvus line during cooling resulted in precipitation of the Cu-rich phases at the boundaries of the Al grains, which is typical behavior for welded V-1461 Al alloy [45]

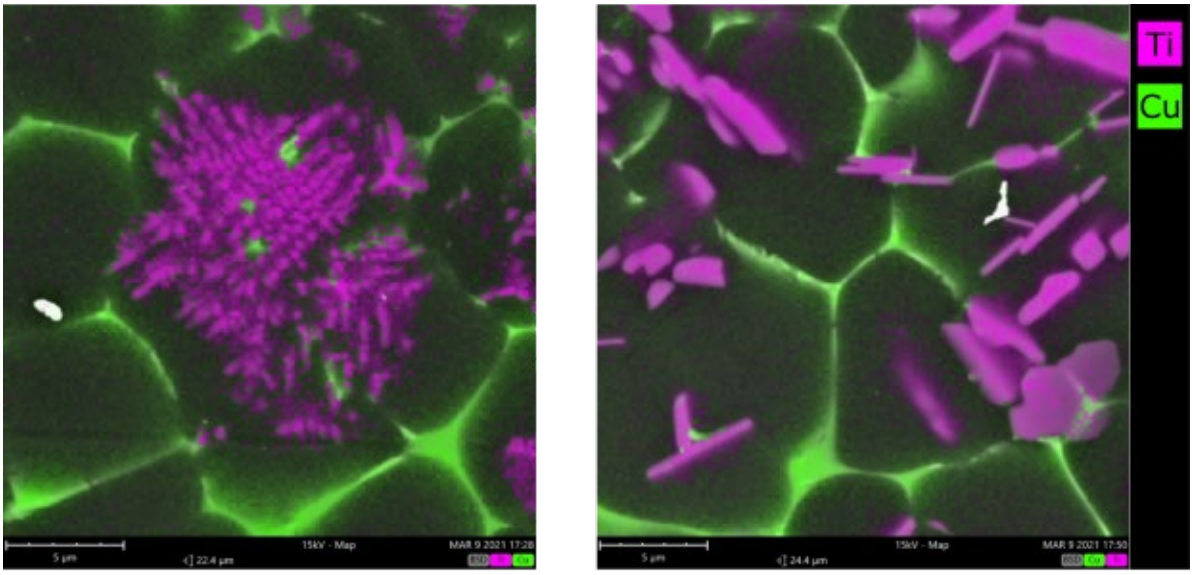

a b

Figure 7 — Structure of the Al FZ (Composition map): a - at its center, b - near border with MZ

The structure of the MZ (Figure 8) is mostly chemically homogeneous (~ 34 at. % Al). However, it also contains rare inhomogeneous areas containing reduced amount of Al to ~ 30 at.% (Figure 8, a; Table 5). High magnification also shows some relief on the polished surface of this zone (Figure 8, b) which can be seen without any etching procedure.

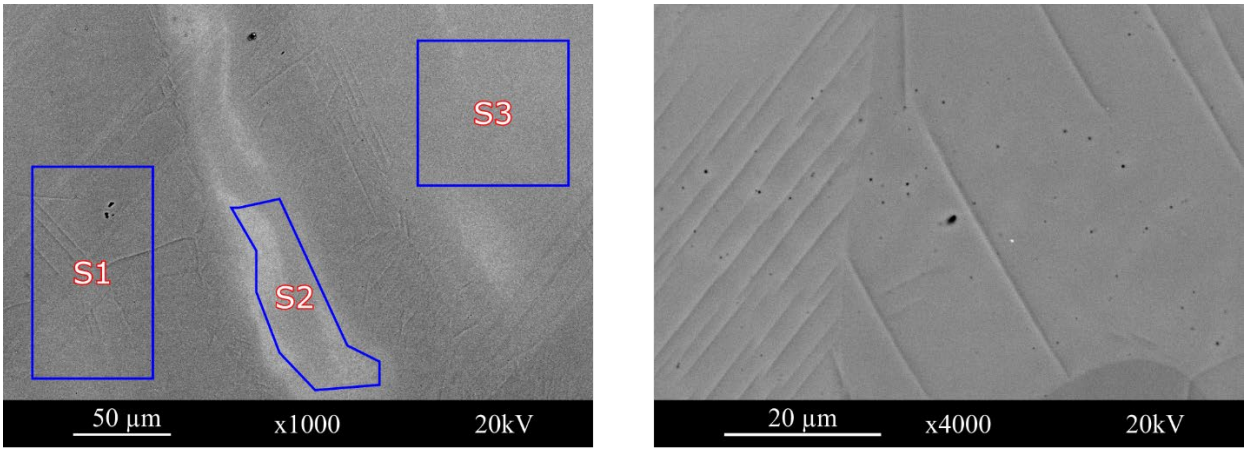

a b

Figure 8 — Structure of the mixing zone: a - composition inhomogeneity in MZ, b - Relief at polished MZ surface

Table 5 — Chemical composition of the areas S1-S3 in Figure 8

Spectrum	Al, at. %	Ti, at. %	Cu, at. %
S1	35.70	63.96	0.34
S2	30.45	69.25	0.30
S3	33.60	66.04	0.36

3.1.2 Welding with beam offset of 0.5 mm

The structure of this joint is similar to the previous case: it also contains 2 different zones, which was melted, but had various crystallization behavior (Figure 9).

The aluminum melting zone, as in the previous case, contains titanium-rich needle-like structures and copper-rich net-like structures surrounding the aluminum grains (Figure 10, a; Table 6). There are also structures richer in titanium (Figure 10, b), with its content in the core of about 45 at.% (Which corresponds to TiAl) and a decrease in the amount of titanium in the shell to 20 at.% (Which corresponds to TiAl3).

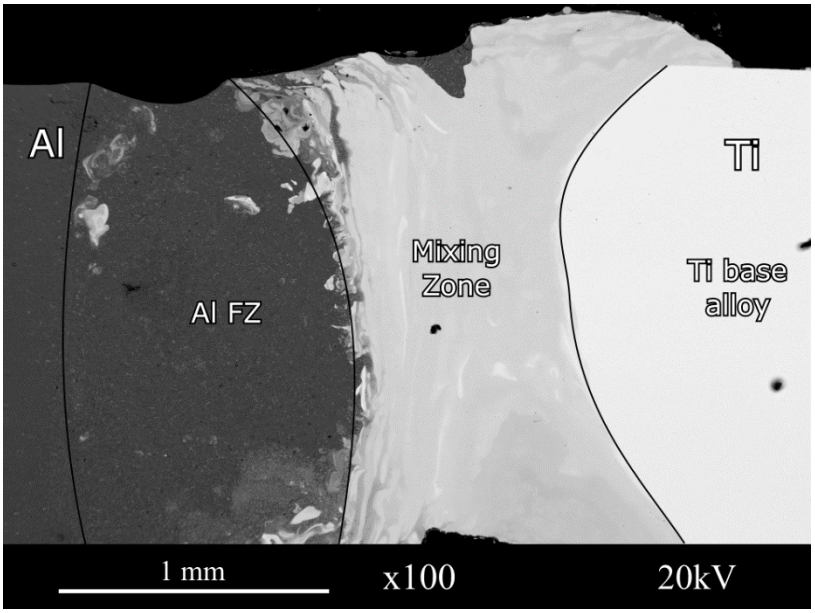

Figure 9 — The main view of the structure of the joint welded with the offset of 0.5 mm

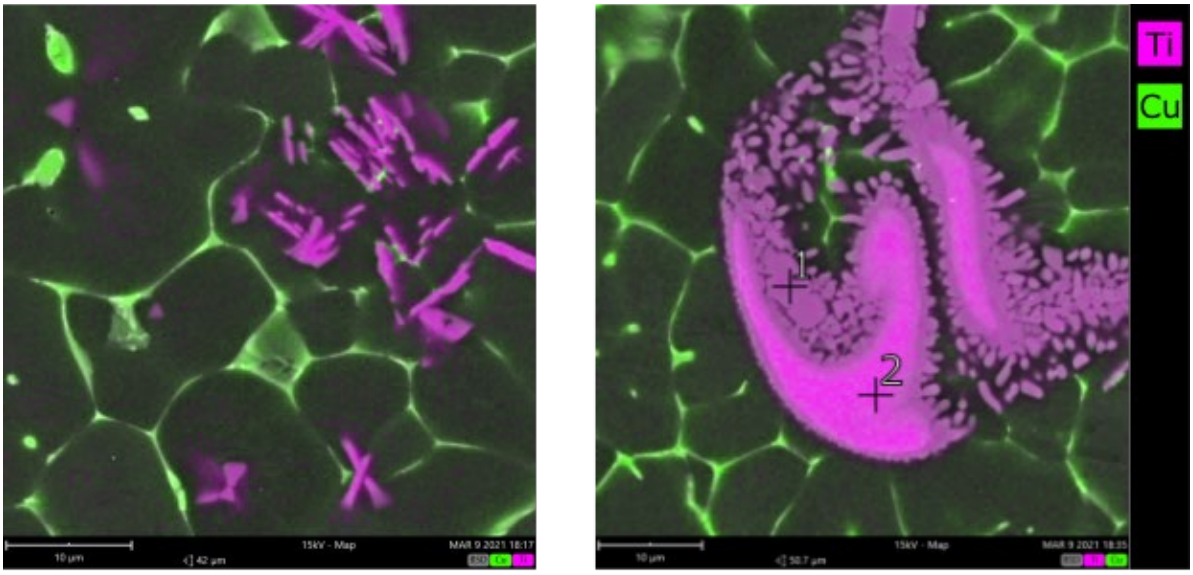

Figure 10 — Structure of the Al FZ (Compositional map): a – needle-like Ti-rich particles, b - Ti-rich particle of other kind

Table 6 — Chemical composition in the spots 1 and 2 (Figure 10)

Spot	Ti, at.%	Al, at.%
1	20.81	79.19
2	43.86	56,14

As at the previous case mixing zone here is mostly chemically homogeneous, hiving rare areas with higher amount of titanium in them (Figure 11;). However, the most part of this zone in this case contains more Al than for welding without offset (~ 40 vs ~ 34 at.%), and the inhomogeneities have much lower Al amount (~20 vs 30 at.%).

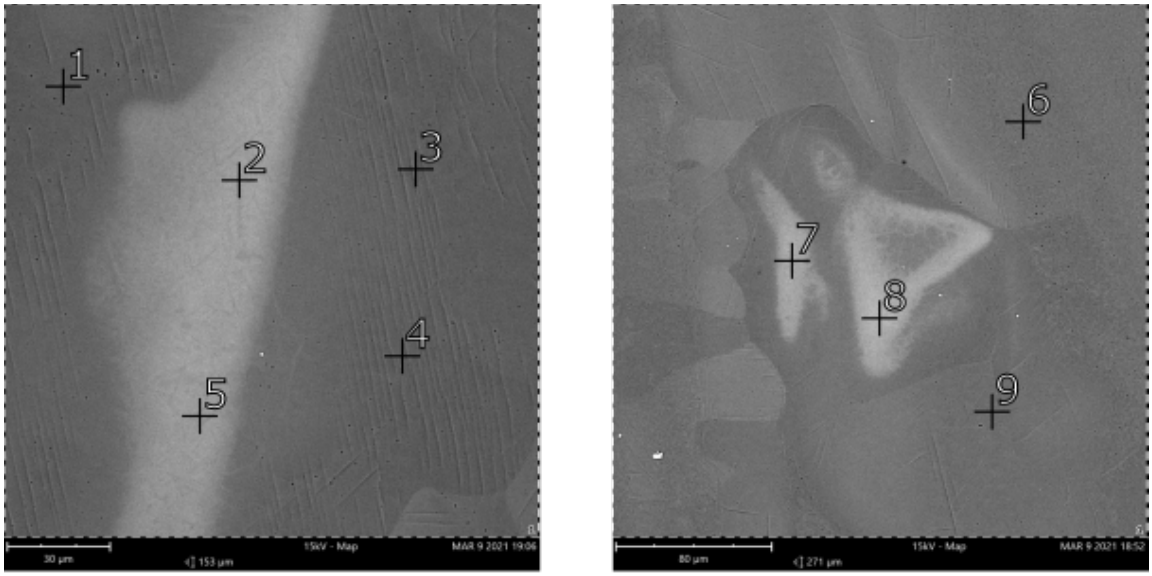

Figure 11 — The composition inhomogeneities and surface relief in the MZ at 2 areas: a – near MZ/base Ti alloy border, b – near Al FZ/MZ border

Table 7 — Chemical composition in the spots 1-9 (Figure 11)

Spot	1	2	3	4	5	6	7	8	9
Ti, at.%	60.62	82.02	61.49	60.88	79.25	57.10	73.34	75.92	58.96
Al, at.%	39.38	17.98	38.51	39.12	20.75	42.90	26.66	24.08	41.04

3.1.3 Welding with beam offset of 1 mm

Welding with the beam displacement of 1 mm allowed to avoid the Ti and Al alloys melts mixing (Figure 12). It happened due to the fact that temperature near the interface between the plates did not reach the melting point of the titanium alloy, so a semblance of a soldered joint was formed, where the aluminum alloy itself served as the solder.

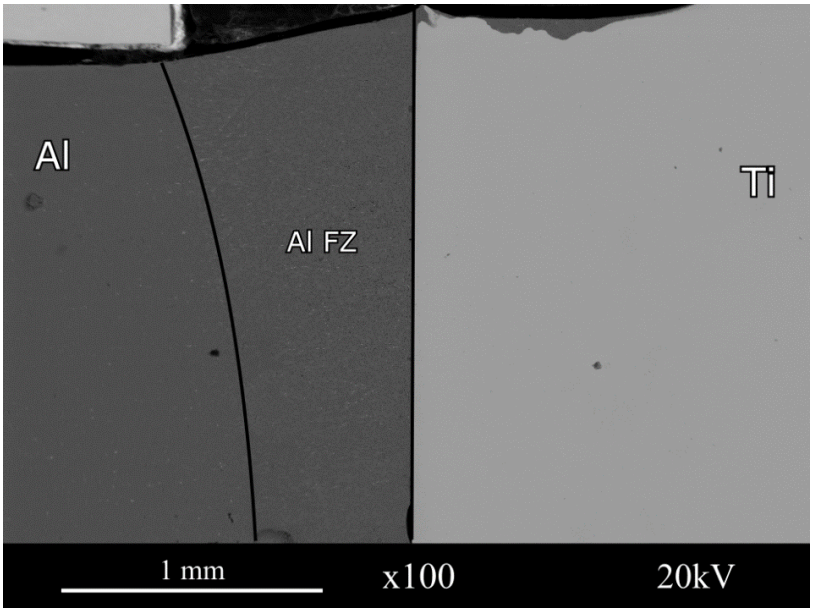

Figure 12 — The main view of the welded with 1 mm offset joint structure

As in the previous cases, the structure of Al fusion zone (Figure 13) contains Cu-rich precipitates at the boundaries of the Al grains, but it doesn't have any structures containing Ti, which indicates the complete exclusion of titanium mixing into this zone.

Structures containing titanium were also not found near the boundary with the titanium plate; however, there is a thin (~ 2 μm) intermetallic interlayer between the plates, which is formed during the interaction of an aluminum melt with solid titanium [2].

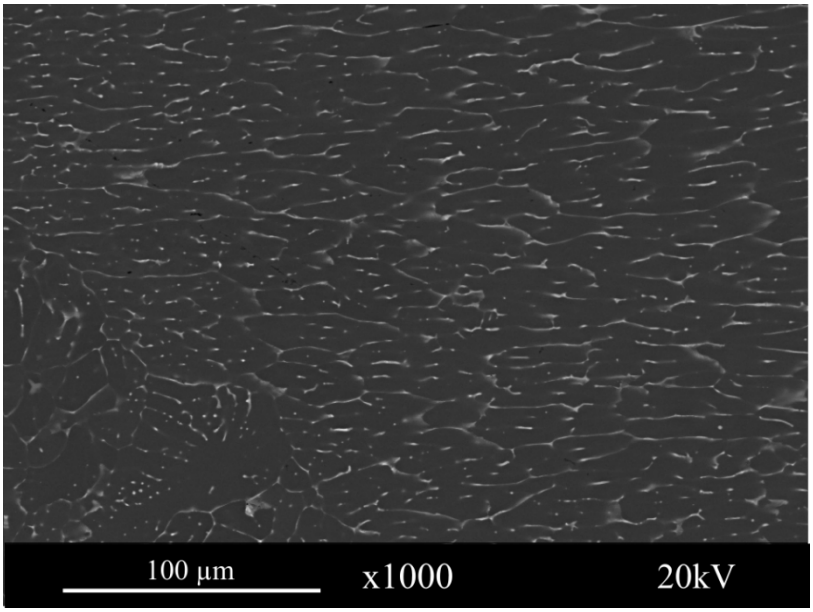

Figure 13 — Structure of the Al FZ at its center

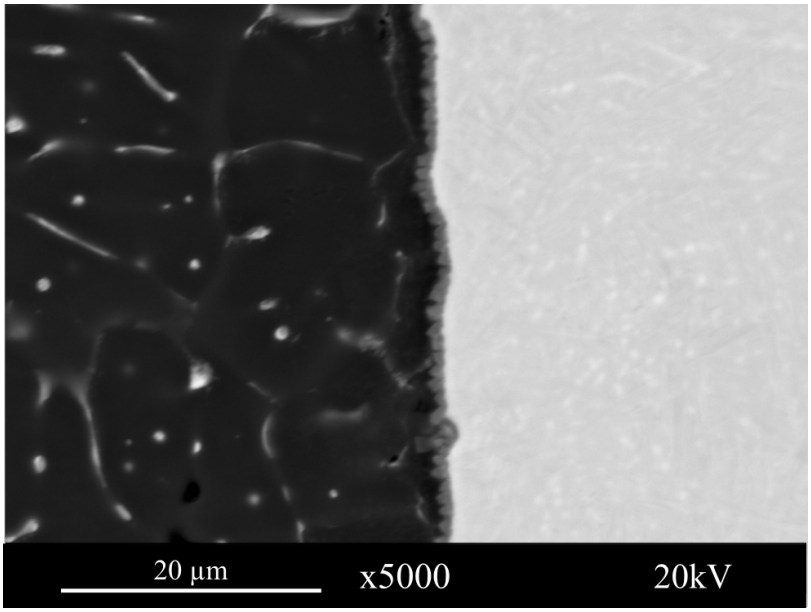

Figure 14 — The boundary structure of the joint

3.2 Tensile tests

Tensile tests have shown (Figure 15) that laser beam displacement has a positive effect on the tensile strength of the resulting joints. The strength of the joints increased from 74 MPa (22.8% of the strength of the V-1461 welded joints [46]) to 168 MPa (51.9% of the strength of the V-1461 welded joints [46]).

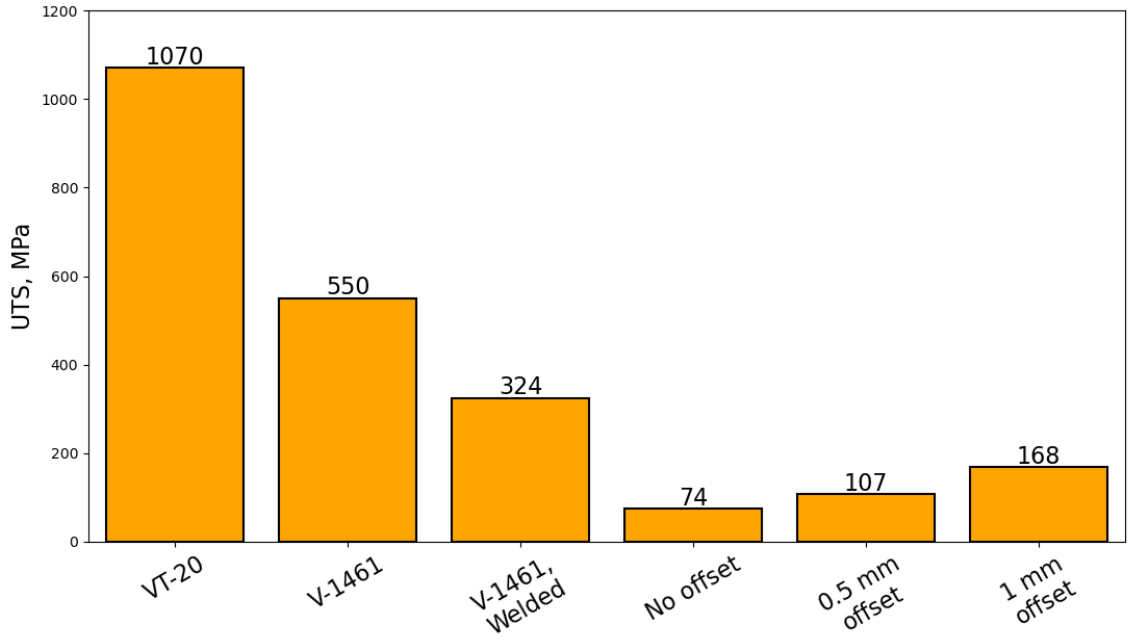

Figure 15 — The tensile tests results comparing with the base materials strength

3.3 Phase analysis

3.3.1 The observed phases description

The synchrotron radiation diffraction analysis showed that the samples contained: α-, α'-, α''- and β-Ti, Al, hardening phases δ'(Al_3Li), T_1, T_2 и T_3 and ordered solid solutions and intermetallic compounds β_2-Ti, α_2Ti_3Al, γTiAl and $TiAl_3$. The information about their symmetry, cell parameters and other information is shown in Table 8.

Table 8 — Phases detected in the Ti/Al weld joints

Phase/ Temperature Range (°C)	**Pearson Symbol/ Space Group/ Prototype**	**Lattice Parameters (pm)**	**Comments**
Al < 660.452	cF4 Fm-3m Cu	a = 404.96 [47]	0 to 0.6 at.% Ti [48]
βTi 1670 - 882	cI2 Im-3m W	a = 330.65	0 to 44.8 at.% Al [47] possible ordering to β_2-Ti [47]
α/α′Ti < 1490	hP2 P63/mmc Mg	a = 295.06 c = 468.35	0 to 51.4 at.% Al [47]
α″	Cmcm	a = 310 b = 490 c = 466	metastable
Ti3Al ≲1164	hP8 P63/mmc Ni3Sn	a = 580.6-574.6 c = 465.5-462.4	~20 to 38.2 at.% Al [49]
TiAl < 1463	tP4 P4/mmm AuCu	a = 400.0-398.4 c = 407.5-406.0	46.7 to 66.5 at.% Al [49]
$TiAl_3$ (l) < 950	tI32 I4/mmm TiAl3 (l)	a = 387.7 c = 3382.8	74.5 to 75 at.%Al [50]
δ′, $LiAl_3$ ≲ 120-190	cP4 Pm-3m Cu3Au	a = 403.8	metastable

τ_3 < 635 Li_3CuAl_5	cI162 Im-3m $Mg_{32}(Zn,Al)_{49}$	a = 1391.4 [51] a = 1390.56 [52]	56.4Al-11.6Cu-32.0Li (at.%) [51] 54.5Al-11.4Cu-34.1Li(at.%) [52]
τ_2, Li_3CuAl_6	quasicrystal	$a = 505\ \tau^{3n}$	τ = gold number = (1 + 51/2)/2, n any integer, point group only m [51,53] 56.0Al-10.8Cu-32.2Li [54]

β-Ti has a body centered cubic (BCC) structure and it is stable at high temperatures (> 882 °C), but it can be stable at room temperature in alloys containing β-stabilizing additives (Cr, Fe, Mo, V et. al.). High amount of aluminum in β-based solid solution may cause ordering of this solution into β_2 phase (Figure 16)

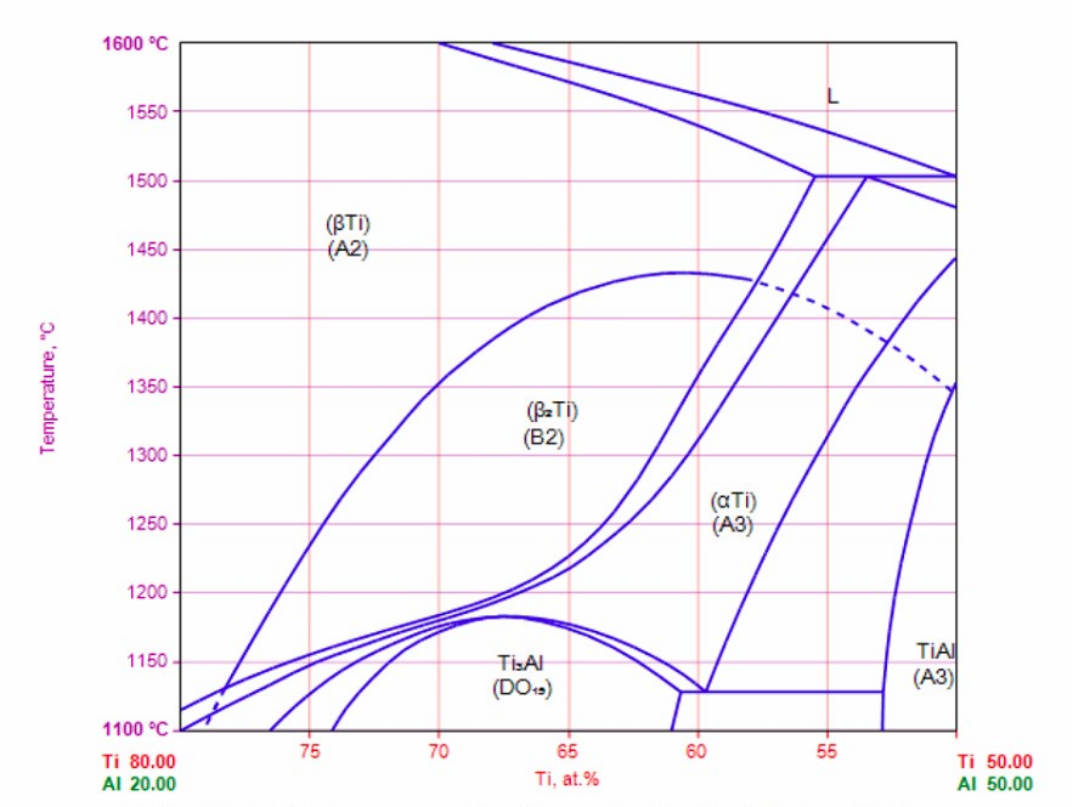

Figure 16 — β_2-Ti in Ti-Al phase diagram

β_2-Ti and α_2Ti_3Al are ordered solid solutions based on β- and α-Ti respectively. α_2 is stable at room temperature without any alloying when β_2 is stable at high temperature (Figure 16). To obtain this phase at room temperature it needs alloying with β-stabilizing elements [55] even with low amount of β-stabilizing elements (~ 3.2 at.% [56]).

γTiAl is an intermetallic compound which appear in Ti-Al systems beginning at ~ 38 at.% of Al. This phase has a tetragonal crystal structure. Like Ti_3Al, γ phase is stable at room temperature.

$TiAl_3$ is also intermetallic compound, which is stable at room temperature, but it has very narrow homogeneity range (from 74.5 to 75 at.% Al [50]).

δ'Al_3Li appears in Al-Li alloys as a result of only quenching [57] or quenching and subsequent artificial ageing [58].

T_1Al_2CuLi is hardening phase which appear in Al-Cu-Li alloys.

Phases $T_3(Al_5CuLi_3)$ and $T_2(Al_6CuLi_3)$ are related. T_3 is a cubic phase, stable under normal conditions, existing in alloys of the Al-Cu-Li system, however, periodic defects in its structure lead to the formation of an icosahedral quasicrystalline structure T_2 [59].

α-Ti is characterized by a hexagonal close-packed (HCP) lattice and is the main (in α + β and pseudo-α alloys) or the only (in α alloys) phase in titanium alloys. High cooling rate may result in formation of α″-Ti instead of α phase. α″ has an orthorhombic structure.

3.3.2 Welding with no offset

During the study the sample was filmed in 7 areas (Figure 17). The first 2 areas were in the Al base alloy (Figure 18). In addition to the reflections of aluminum, weak reflections of the strengthening phases T_1 and T_3 are observed. Reflections of the quasicrystalline structure T_2 formed in T_3 are also observed. Since T_3 does not have a clear crystal structure, indexing of its peaks is not possible. Since the size and proportion of the particles are extremely small, the reflections are broadened and of low intensity, which can only lead to the observation of the strongest of them.

The third section (Figure 19) was located in the heat affected zone, where the hardening phases precipitated at the grain boundaries, as a result of which the particle size increased. Due to this, their reflexes became sharper and more obvious.

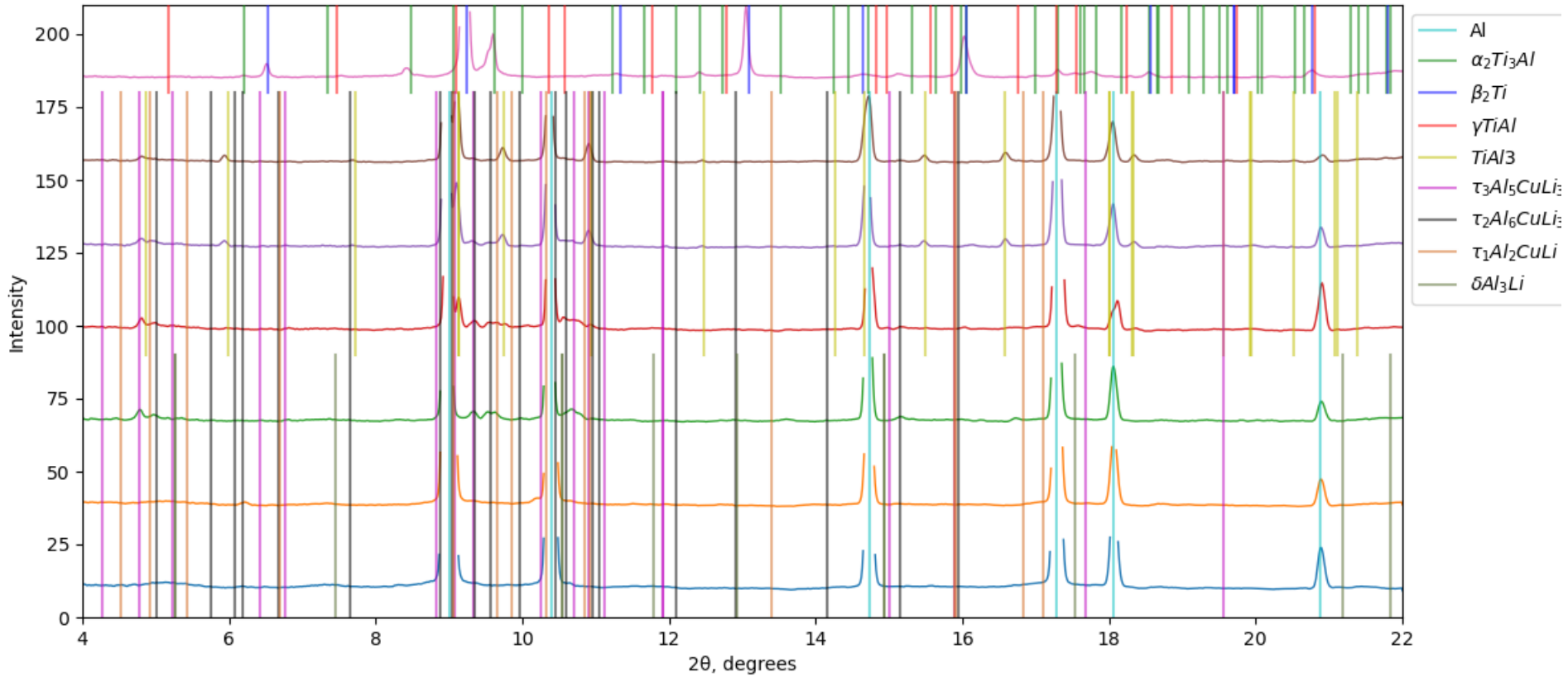

Figure 17 — Synchrotron X-ray diffraction spectra of the welded without laser offset joint from the Al alloy to the Ti one (from below to above)

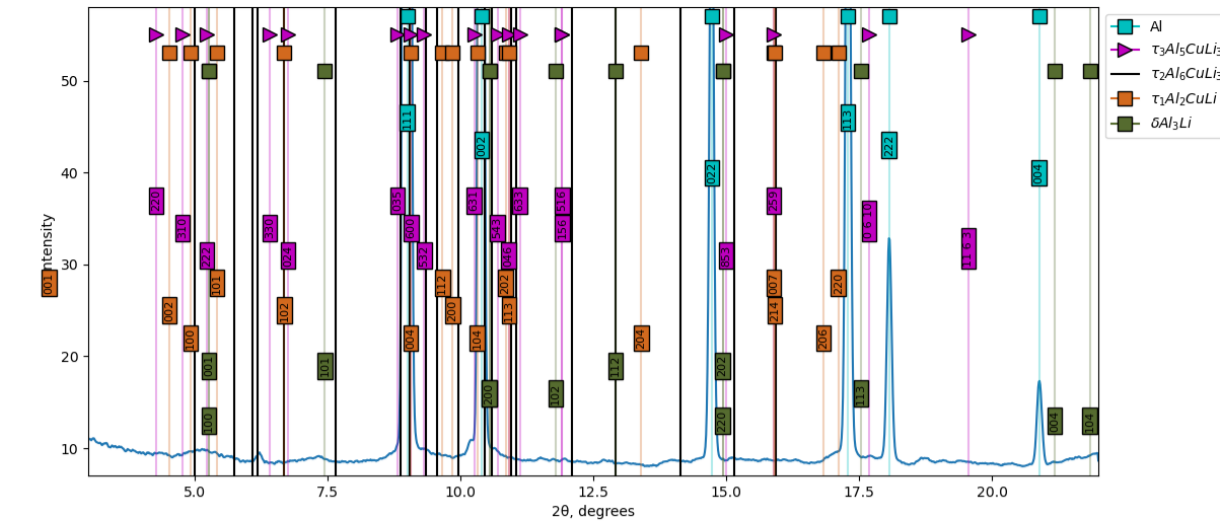

a

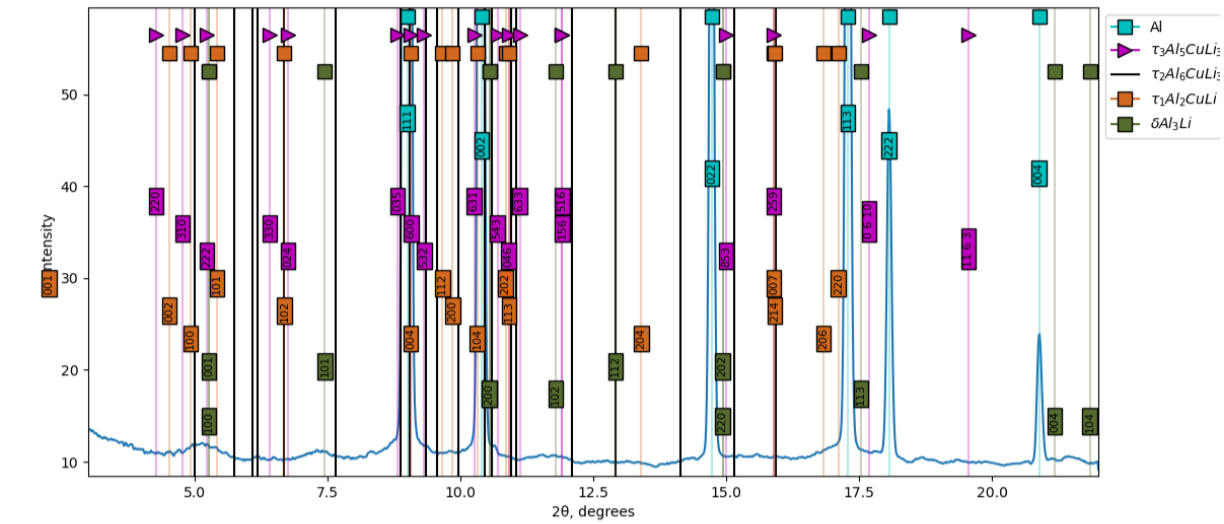

b

Figure 18 — Synchrotron X-ray diffraction spectra of the base Al alloy: a – spectrum 1; b – spectrum 2

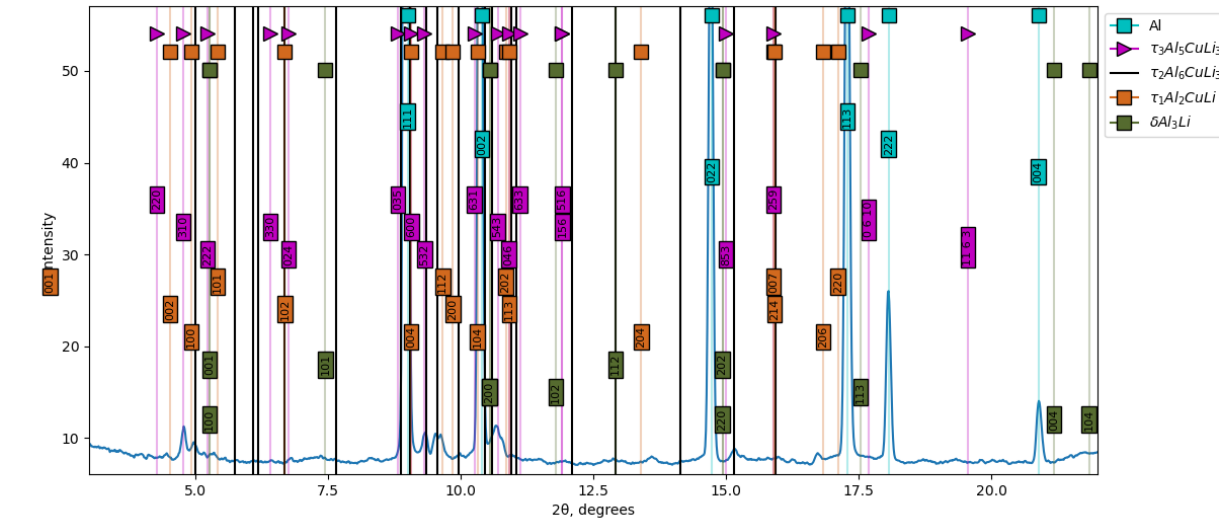

Figure 19 — Synchrotron X-ray diffraction patterns of heat affected zone in Al

The fourth and the fifth sections belong to Al FZ (Figure 20), which also contains reflections of strengthening phases, but reflections of TiAl3 are also observed. It can be also noticed that the δ' reflexes have disappeared or become too weak to be observed.

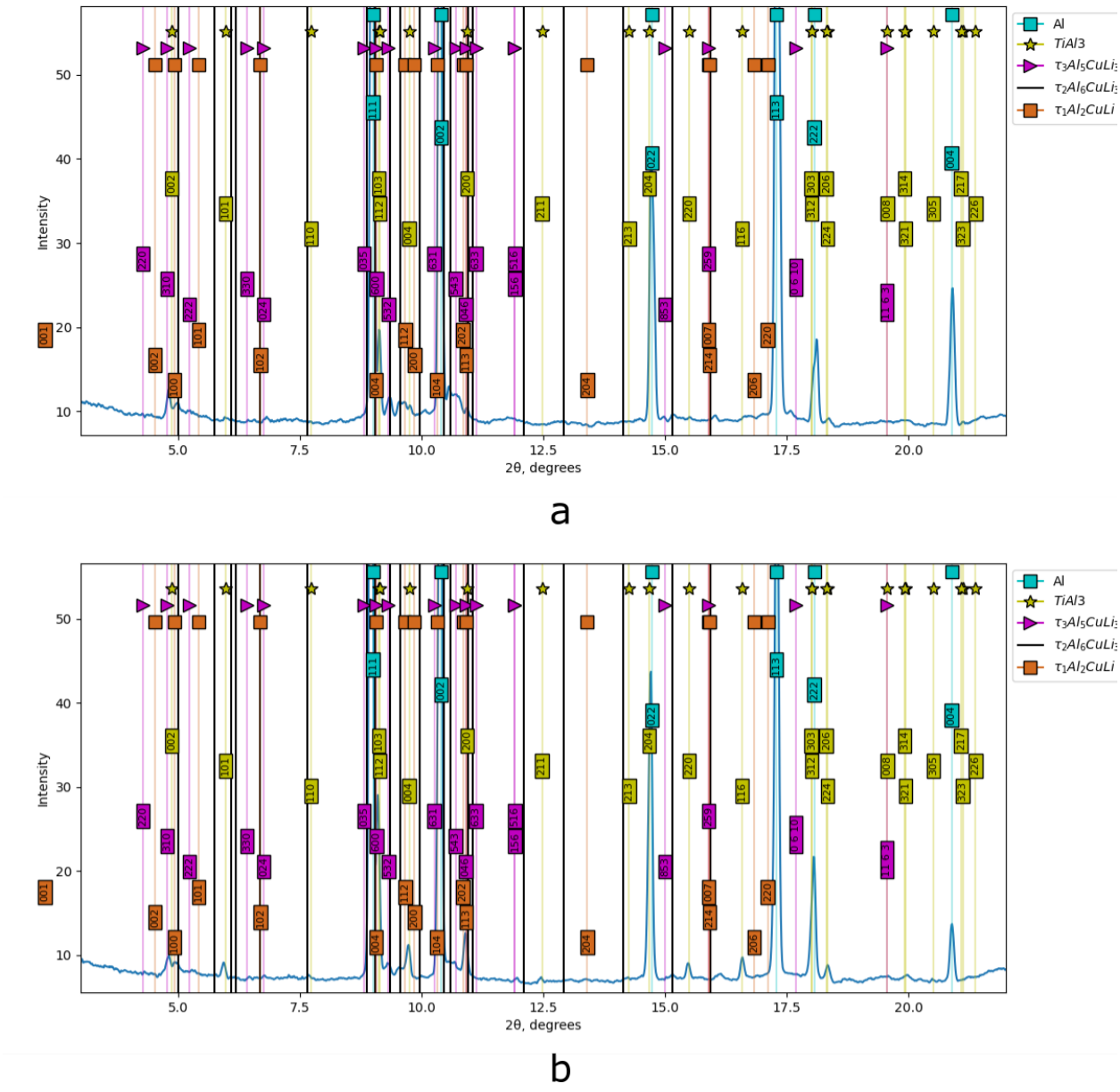

Figure 20 — Synchrotron X-ray diffraction patterns of the Al FZ: a – the 4th section; b – the 5th section

EDX analysis showed (Figure 8) the aluminum concentration corresponding to the α_2Ti3Al phase in the MZ, which was confirmed by diffraction of synchrotron radiation, however, γTiAl and β_2-Ti reflections are also present in the image of this region (Figure 21).

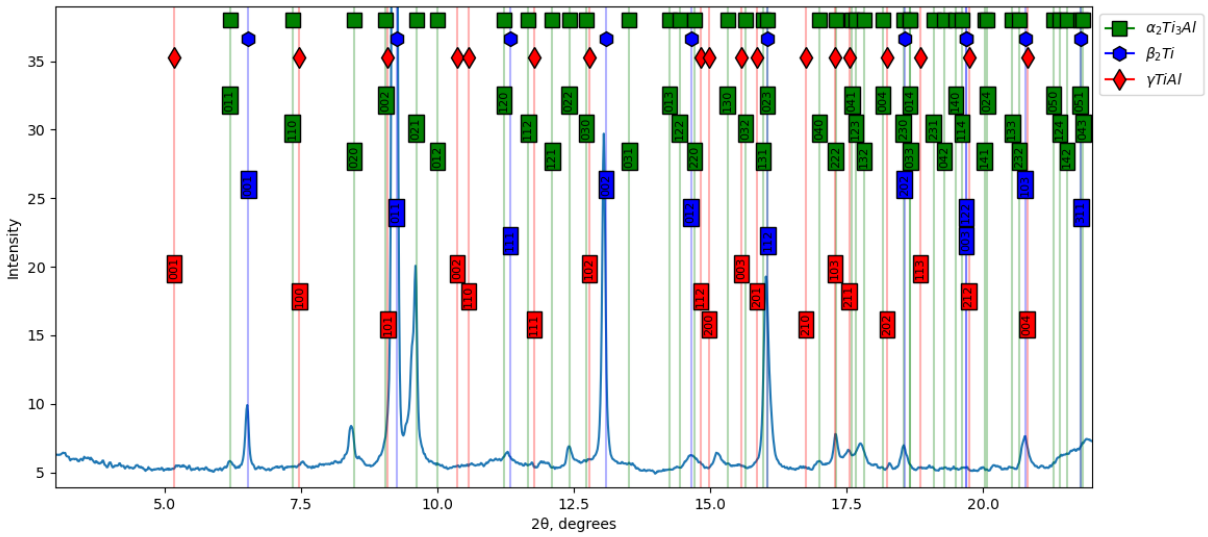

Figure 21 — Synchrotron X-ray diffraction patterns of the MZ

3.3.3 Welding with offset of 0.5 mm

As in the previous case, this sample was filmed in 7 areas (Figure 22), moving from the base titanium alloy through the weld to the aluminum alloy.

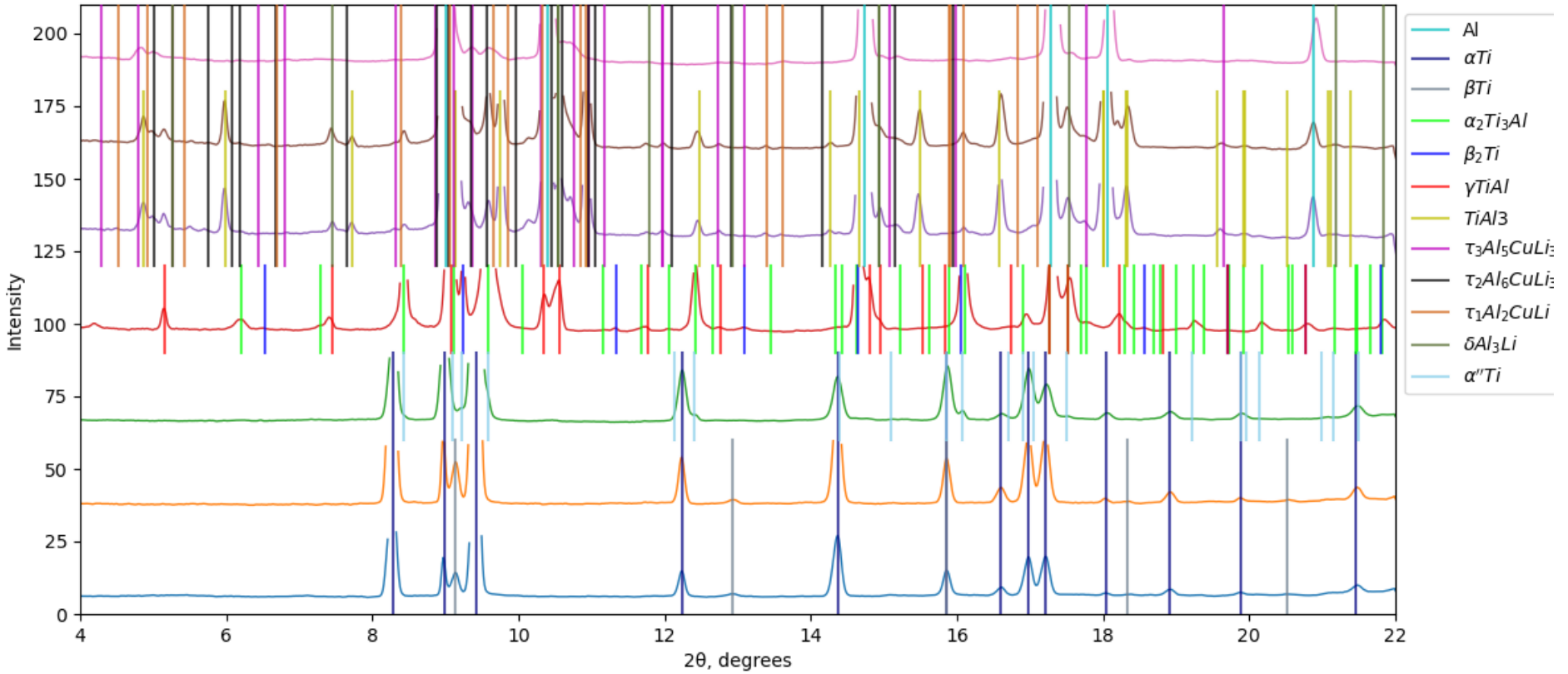

Figure 22 — Synchrotron X-ray diffraction patterns of the weld joint (laser offset of 0.5 mm to Ti) from the Ti alloy to the Al HAZ (from below to above)

The first 2 images belong to the base titanium alloy (Figure 21). Reflections of α- and β-Ti can be observed here, which corresponds to the class of the selected titanium alloy.

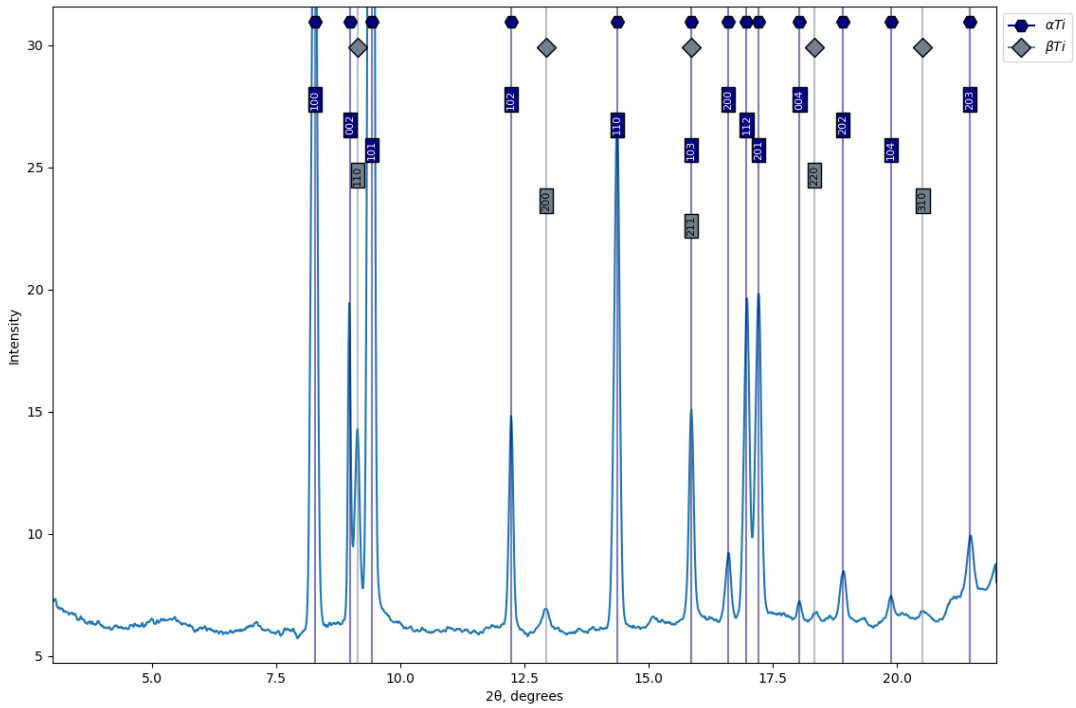

a

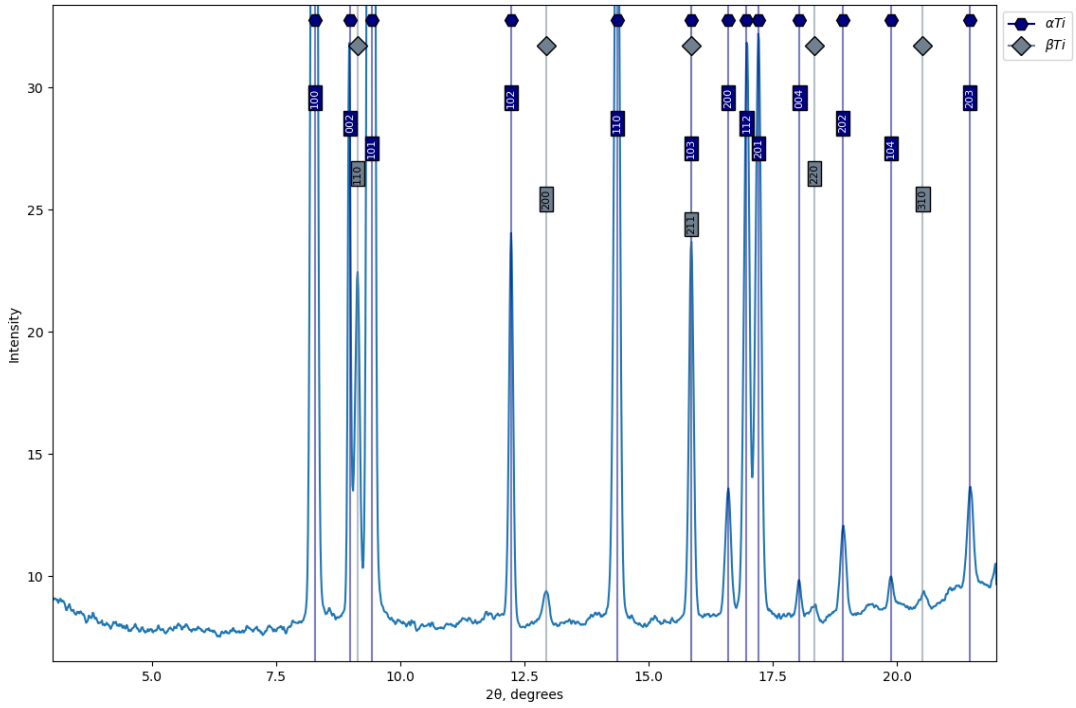

b

Figure 23 — Synchrotron X-ray diffraction patterns of the base Ti alloy: a – the 1st section, b – the 2nd section

Rapid heating and subsequent cooling near the welding zone, characteristic of laser welding, led to the appearance of martensitic structures. From the diffraction of synchrotron radiation in this region (Figure 24), it can be said that welding led to the appearance of α'- and α''-Ti structures.

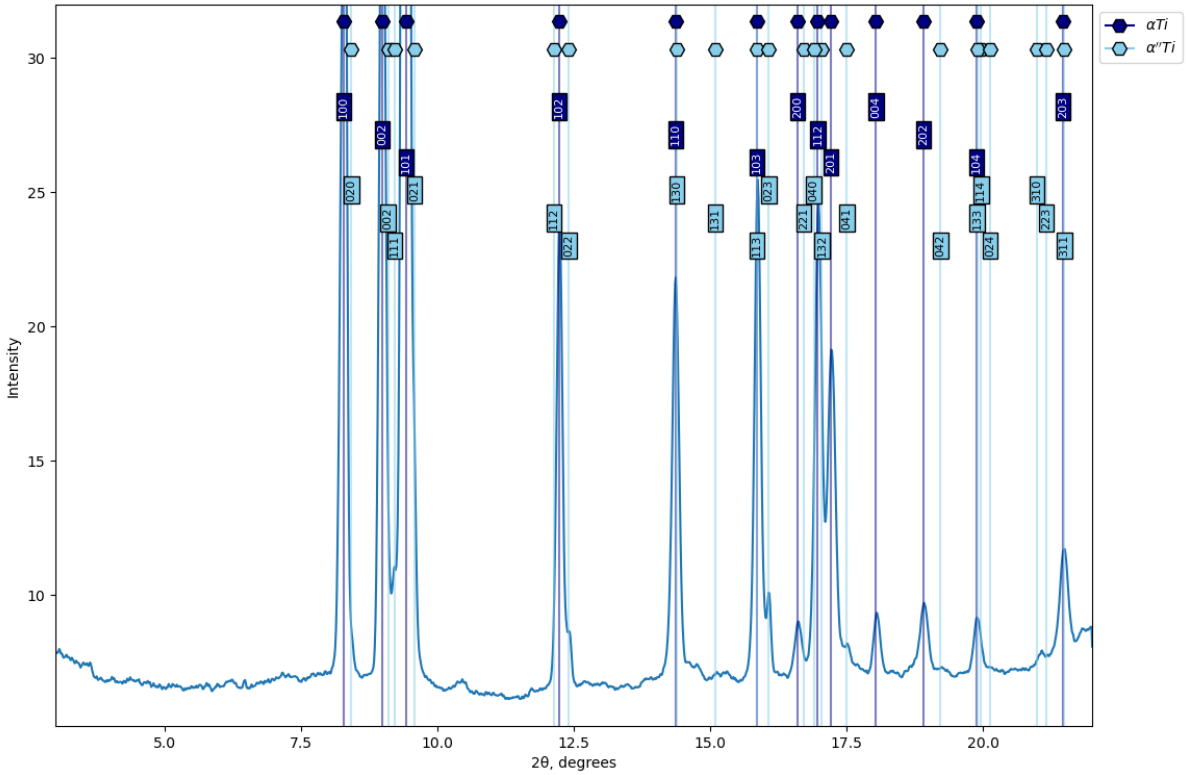

Figure 24 — Synchrotron X-ray diffraction patterns of the heat affected zone

The mixing zone in this sample differed from the previous case by an increased amount of aluminum in the mixing zone, which led to the formation of a larger amount of the TiAl phase (Figure 25), as evidenced by an increase in the intensity of its reflections. Also, β_2-Ti reflections are less intense comparing with the previous sample.

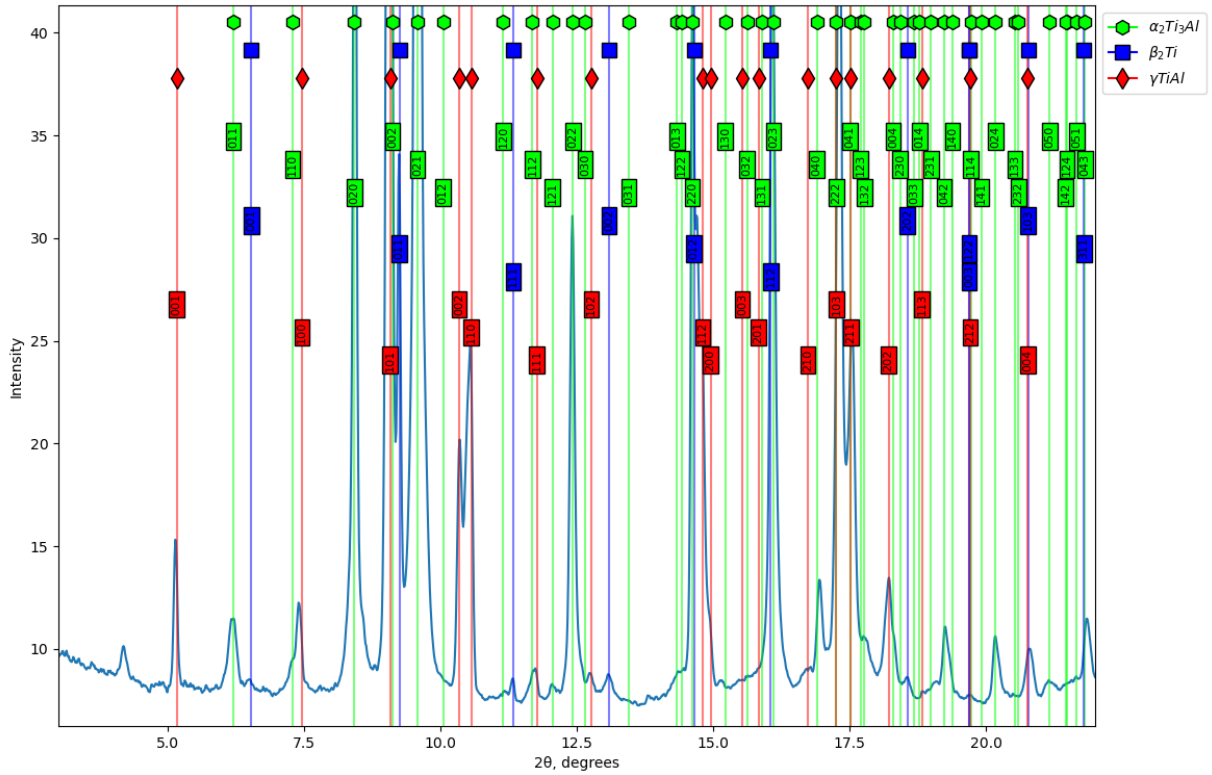

Figure 25 — Synchrotron X-ray diffraction patterns of the mixing zone

The next 2 spectra (Figure 26) refer to Al FZ. The images show reflections of the $TiAl_3$, δ', T_1, T_2 and T_3 phases. As in the previous sample, melting and subsequent crystallization led to the precipitation of strengthening phases at the grain boundaries of aluminum, increasing the zones of coherent scattering in them. Thanks to this, it became possible to observe a larger number of peaks of these phases in comparison with the original material.

The last image (Figure 27) corresponds to the heat-affected zone in an aluminum alloy, where the heating led to the recrystallization of aluminum grains and the precipitation of hardening phases at the grain boundaries, due to which most of their reflections can be recorded.

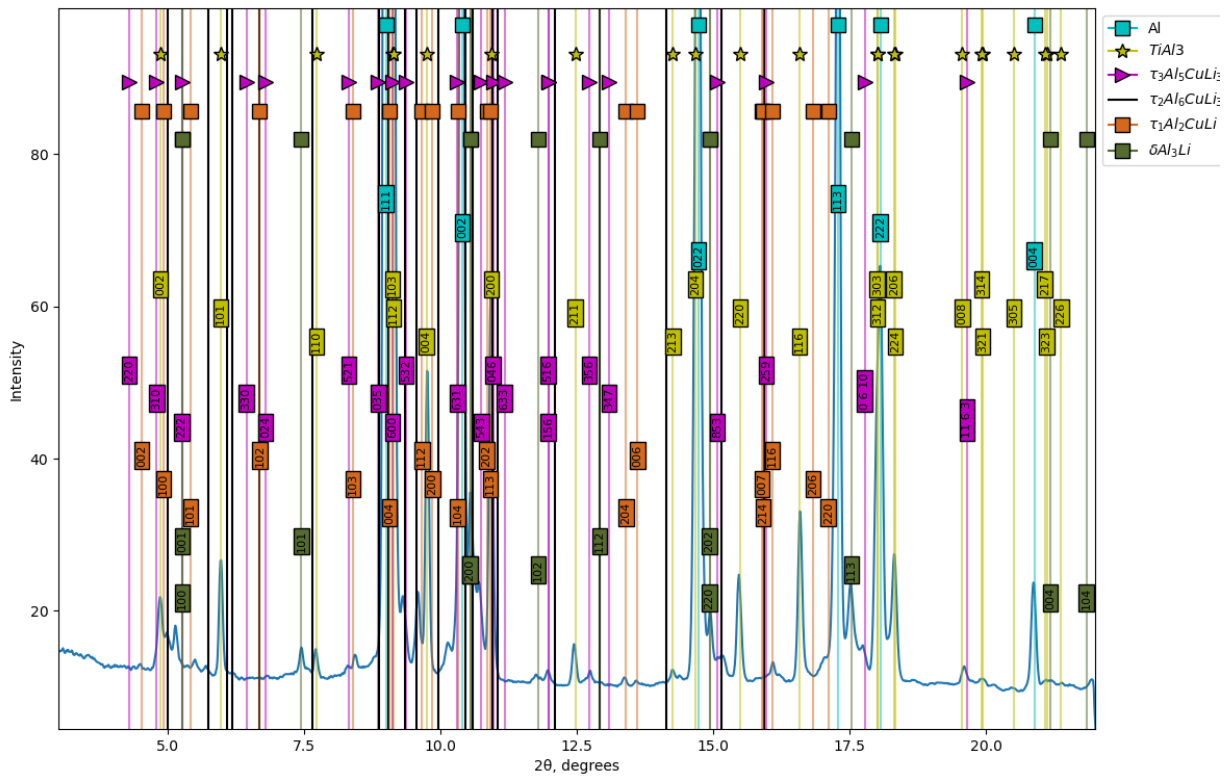

a

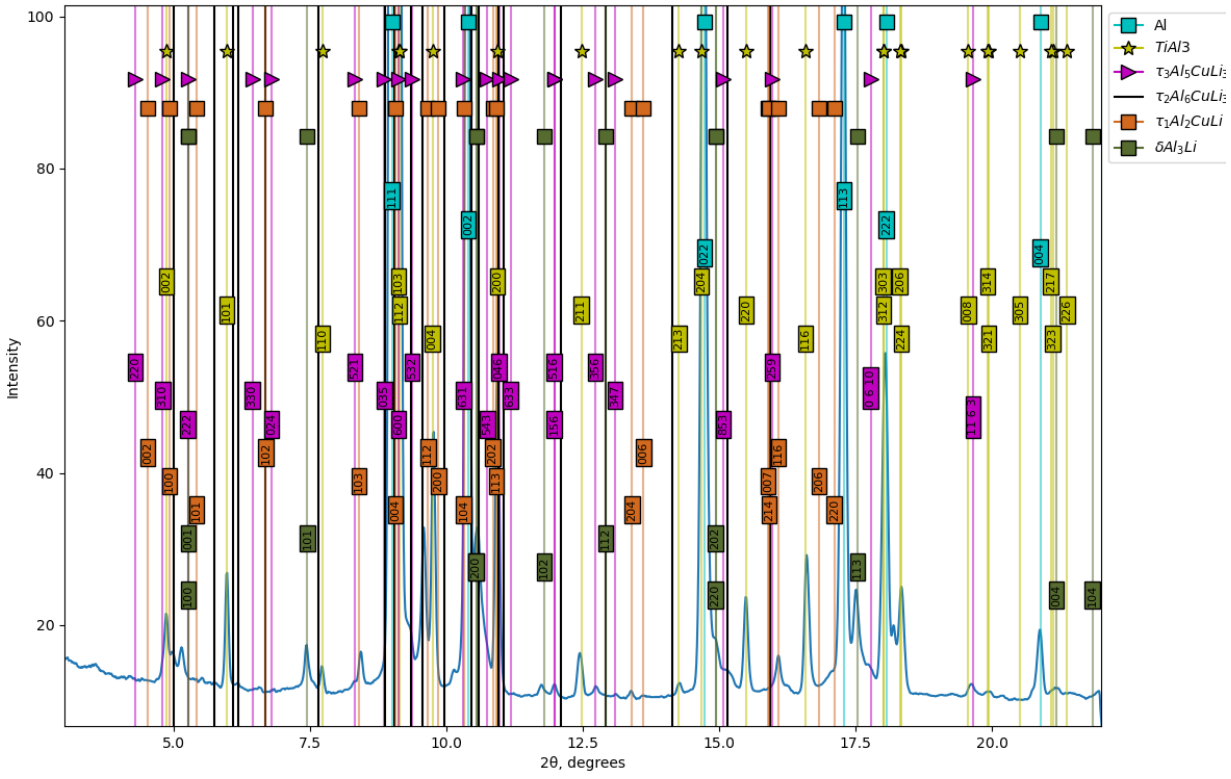

b

Figure 26 — Synchrotron X-ray diffraction patterns of the Al FZ: a – the 5th section, b – the 6th section

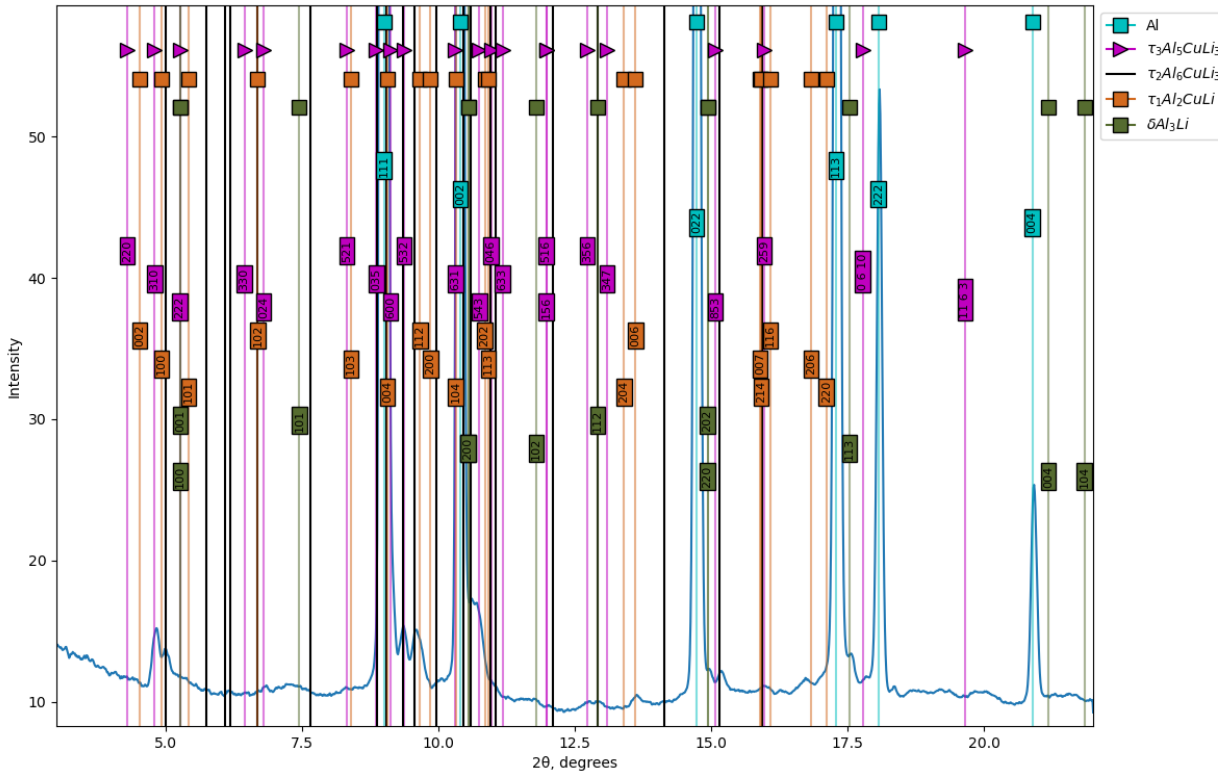

Figure 27 — Synchrotron X-ray diffraction patterns of the HAZ in Al

3.3.4 Welding with offset of 1 mm

The sample was filmed in 5 areas. Unlike previous samples, synchrotron radiation diffraction analysis did not reveal any intermetallic phases other than those in the base materials (Figure 28).

Reflexes of the hardening phases in the heat-affected zone and the melting zone of aluminum (Figure 29) have a less pronounced shape compared to the previous cases, but more pronounced compared to the base alloy.

Laser treatment led to the formation of quenched structures in titanium, which can be seen in Figure 30. Reflections of the retained β-phase were also found in this area.

The last spectrum (Figure 31) refers to the base titanium alloy. SRDA showed phase composition, standard for this Ti alloy

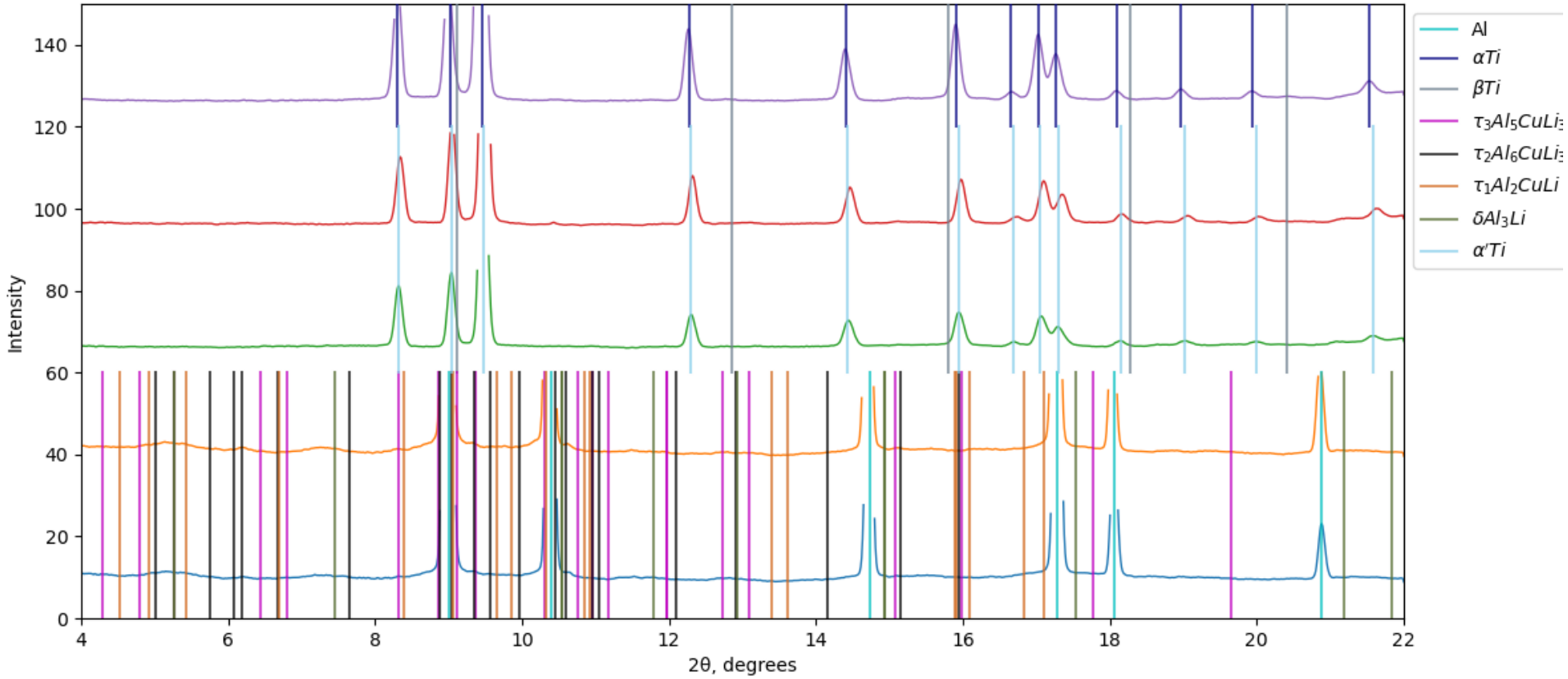

Figure 28 — Synchrotron X-ray diffraction patterns of the weld joint (laser offset of 1 mm to Ti) from the Al HAZ to the Ti alloy (from below to above, logarithmic scale)

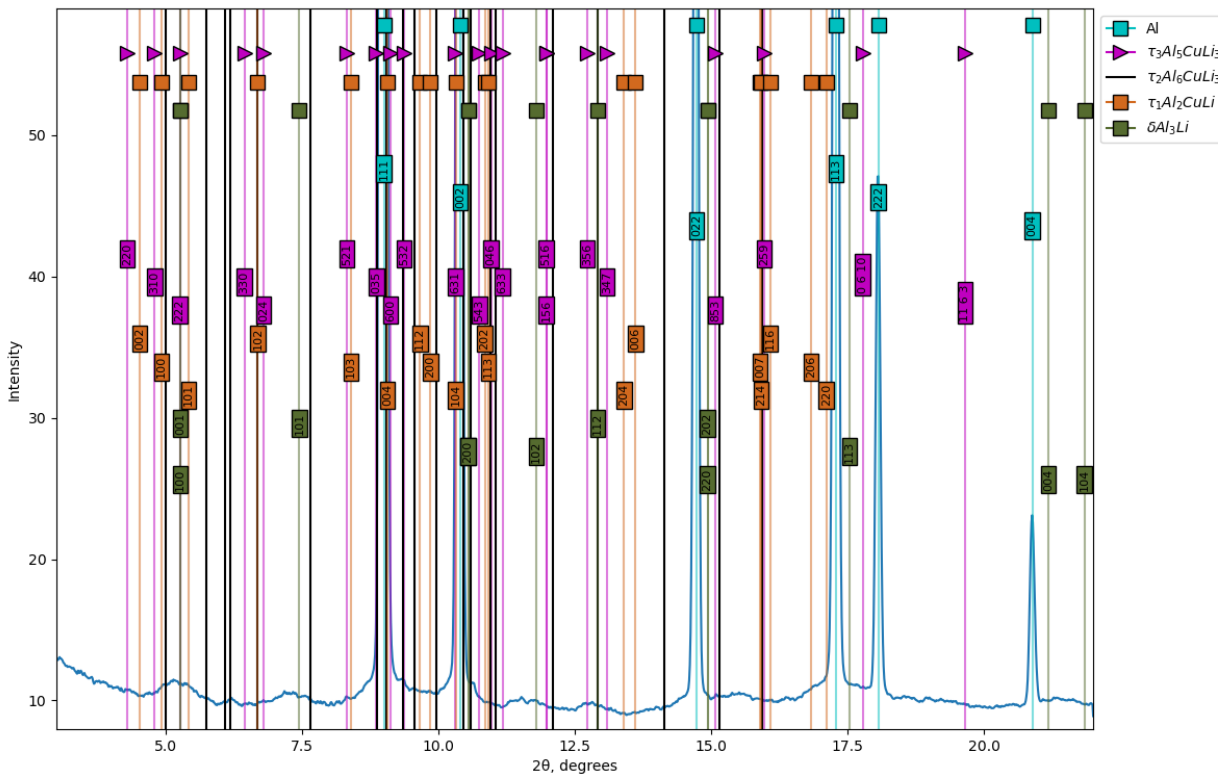

a

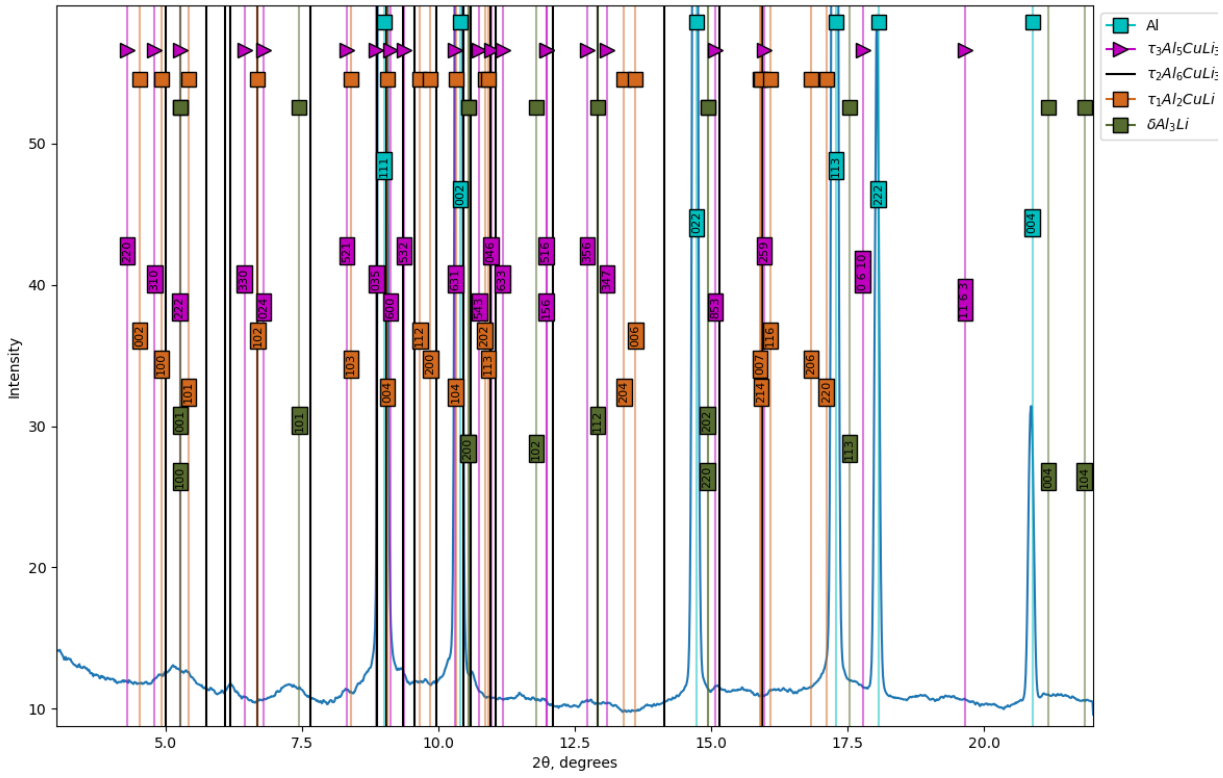

b

Figure 29 — Synchrotron X-ray diffraction patterns of the HAZ in the Al alloy and the Al FZ: a – the 1st section, b – the 2nd section

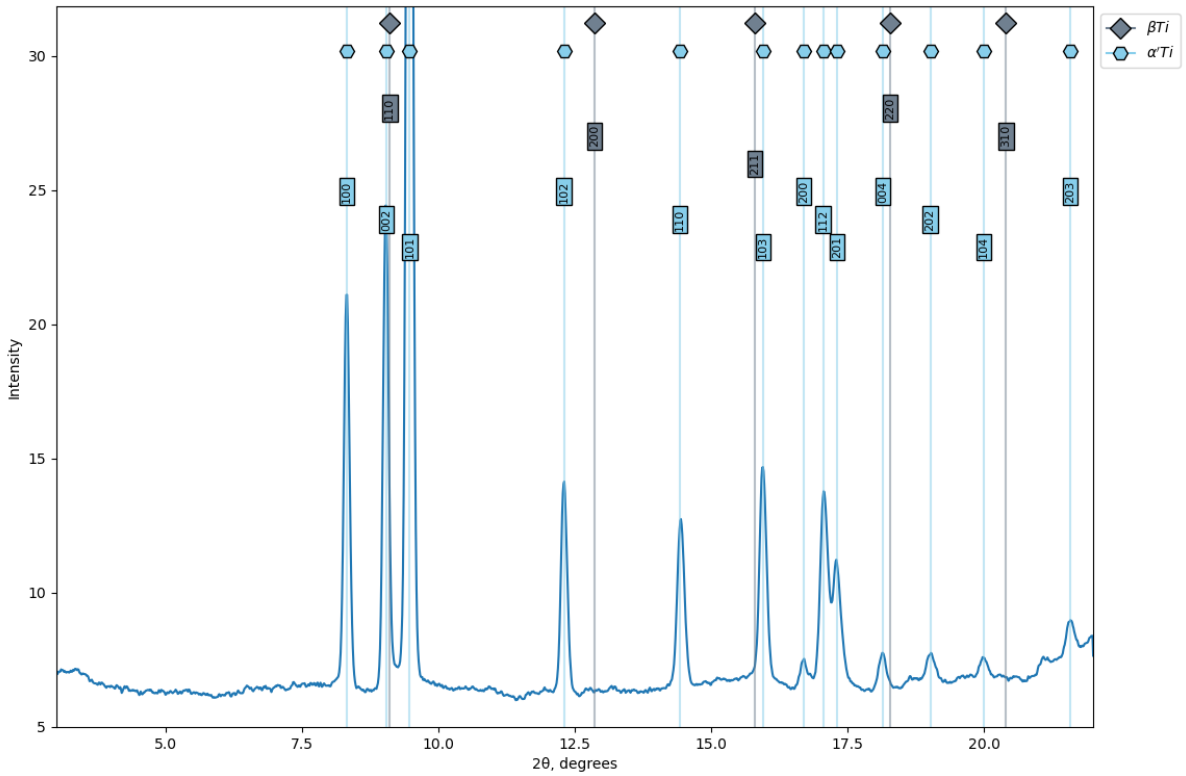

a

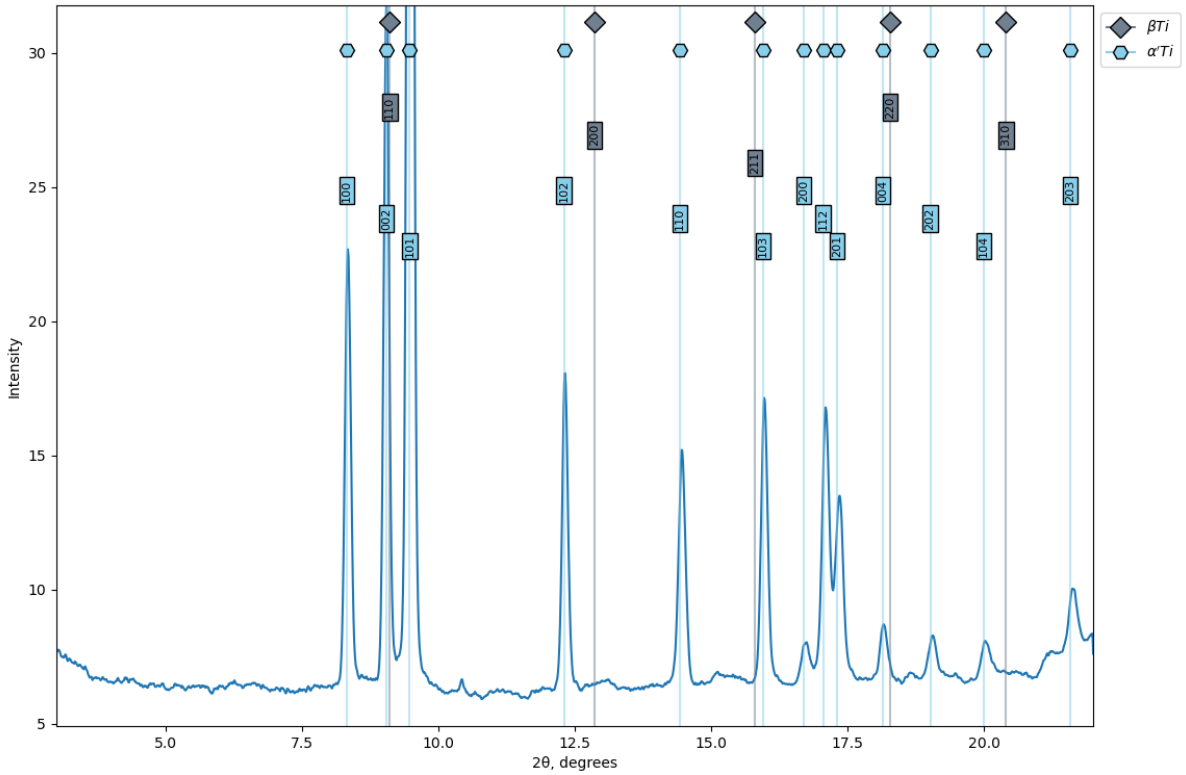

b

Figure 30 — Synchrotron X-ray diffraction patterns of the FZ in the Ti plate: a – the 3rd section, b – the 4th section

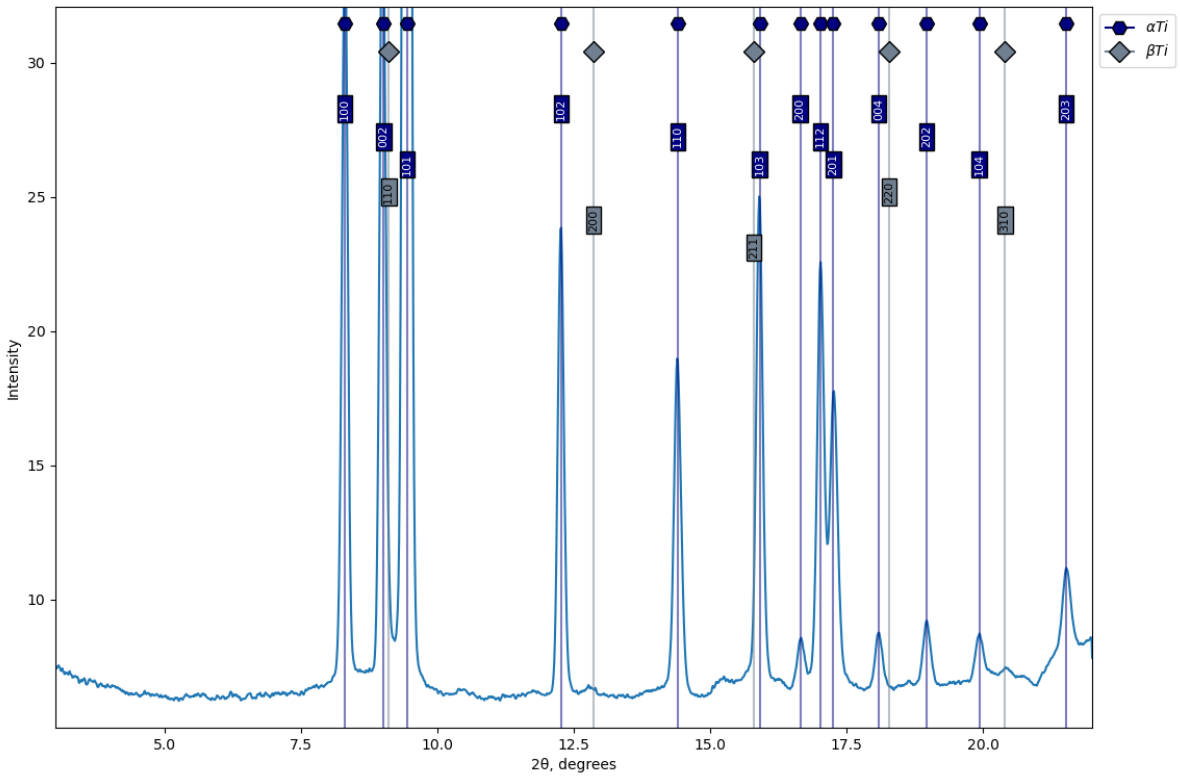

Figure 31 — Synchrotron X-ray diffraction patterns of the base Ti alloy

3.4 Discussion

The research results made it possible to identify several typical structures in the obtained joints.

A typical structure for aluminum alloys of the Al-Cu-Li system (Figure 32) is presented in the form of a matrix of elongated grains of aluminum, in the volume of which precipitates of strengthening particles are observed, which are released through quenching and subsequent artificial aging.

Heating above the solvus temperature led to the dissolution of copper-containing hardening phases, due to which subsequent cooling below this temperature led to the precipitation of these phases at the grain boundaries (Figure 33).

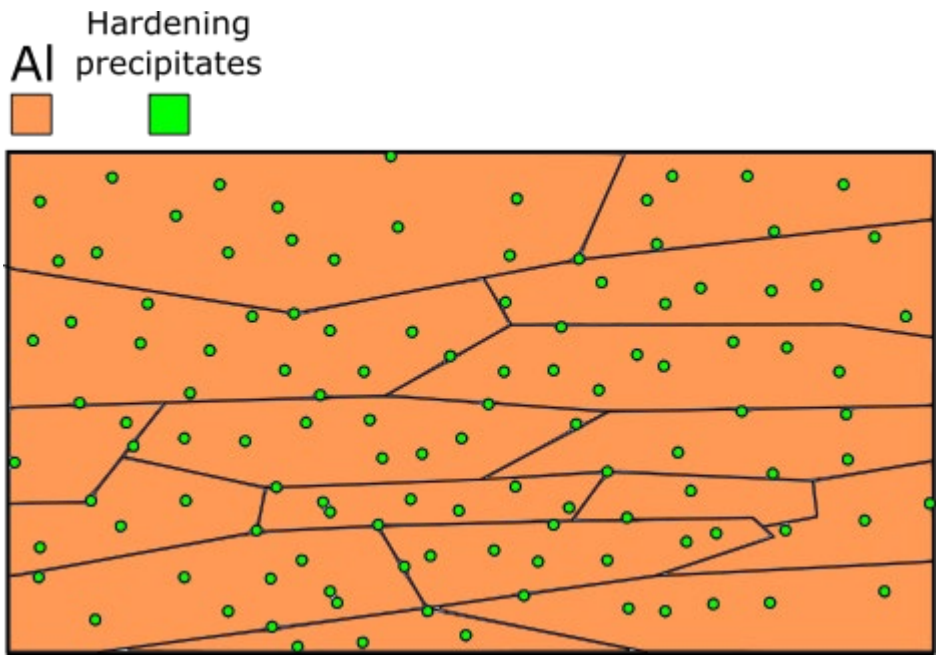

Figure 32 — Typical V-1461 alloy structure scheme

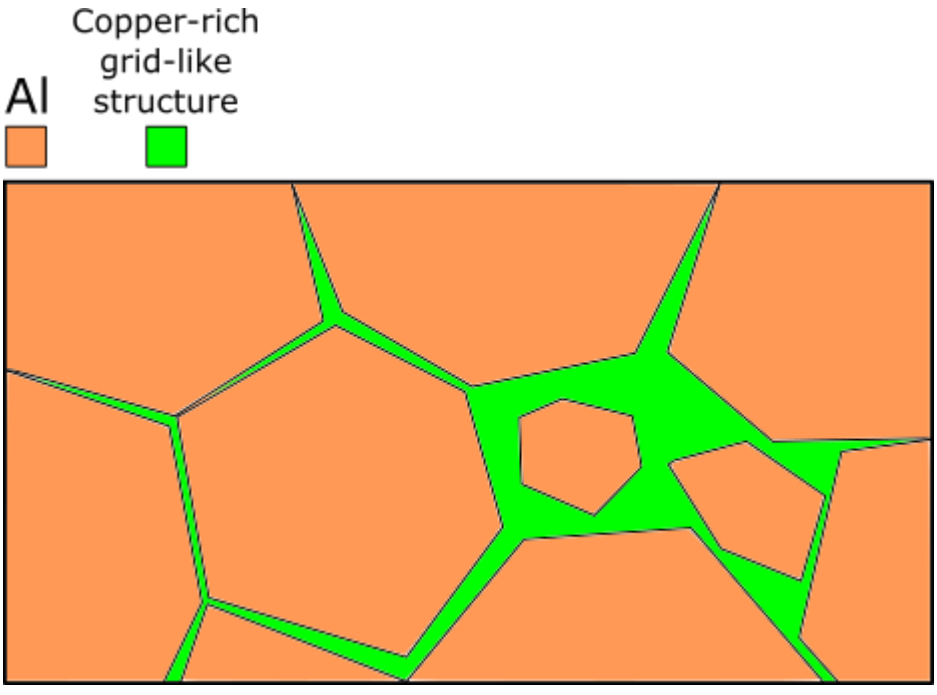

Figure 33 — Heat affected zone structure scheme of the Al alloy

Mutual contact of titanium and aluminum melts during welding led to the fact that part of the aluminum melt, although not fully mixed with titanium, captured part of it, which is why TiAl3 crystals can be observed in the structure of this zone. Since the base alloy was completely remelted, the hardening phases precipitated at the grain boundaries, depriving the aluminum matrix of hardening (Figure 34).

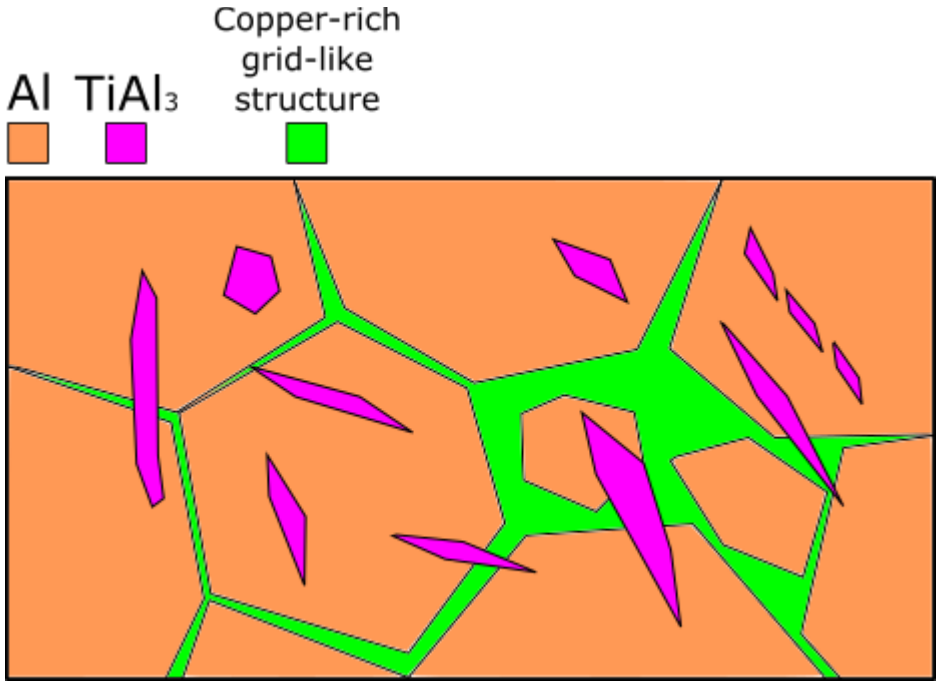

Figure 34 — The structure of the fusion zone in the Al alloy (welding with the offset of 0 and 0.5 mm; scheme)

The alloys melts mixing occurred during welding without displacement and at displacement by 0.5 mm. Although EDX analysis showed differences in the chemical composition of the mixing zone in these samples, their structure is similar (Figure 35). Despite scanning electron microscopy revealed only grains and slip bands (which appear as a result of plastic deformation of Ti_3Al crystals on their surface [60]), phase analysis in both cases showed that these zones also contain β_2 and γ phases. Since the cooling of the system with such an amount of Al from the melt passes through the crystallization of β-Ti (with subsequent ordering into β_2),

the formation of the γ phase and the further transformation of the remaining part of the β phase into α_2, it can be assumed that the TiAl phase is inside the observed grains in the form of thin plates (which is typical for $\alpha_2 + \gamma$ alloys), the size of which does not allow them to be seen with the used detector. Since cooling cannot proceed without the appearance of thermal stress, the grains are deformed, which is why slip bands can be observed on their surface [60].

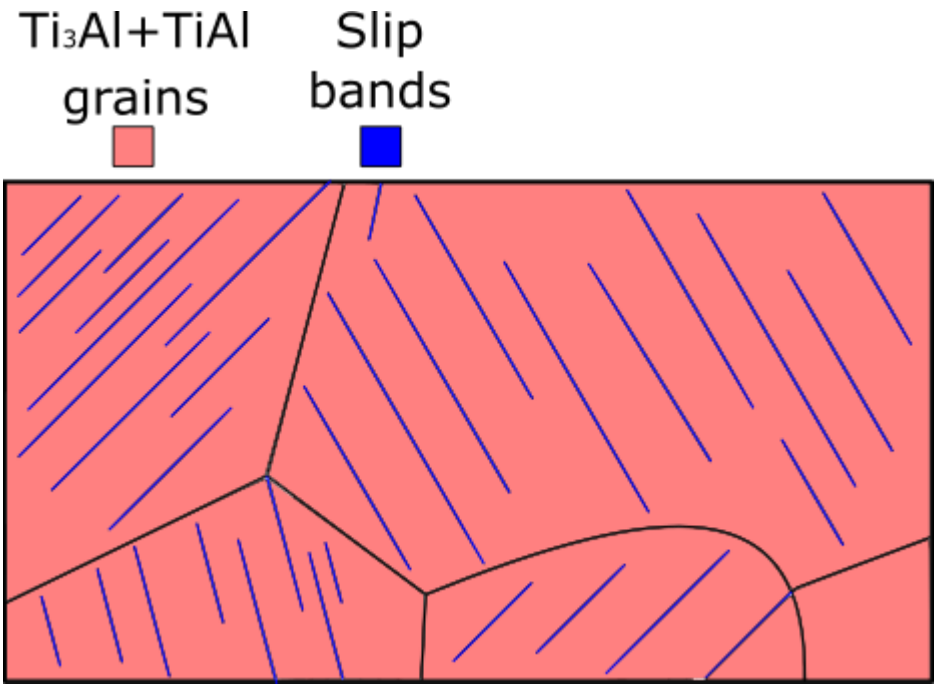

Figure 35 — The structure of the mixing zone (welding with the offset of 0 and 0.5 mm; scheme)

When welding with a displacement of 1 mm, it was possible to avoid contact of the melts, due to which brittle zones consisting of intermetallic compounds were not formed in the structure of the joint, which made it possible to increase the strength by more than 2 times. However, the softening that occurs in the heat-affected zone and the melting zone in aluminum does not allow to achieve high strength values close to the aluminum alloy in the initial state.

3.5 Conclusions

According to the obtained results it can be concluded that:

1. Laser beam offset towards Ti plate during laser dissimilar welding of Ti alloy VT-20 and Al alloy V-1461 results in an increase in the joint strength from 76 MPa to 168 MPa which is 51.9% of the strength of the V-1461 welded joints.

2. The beam displacement leads to significant change in resulting structure of the joints, excluding large interlayer formation (consisting of brittle components – Ti_3Al and TiAl intermetallics). Instead of this a thin (~2 μm) $TiAl_3$ interlayer appears at the boundary between the plates.

3. The Al alloy remelting leads to the material softening in fusion zone of the Al plate, which results in significant strength decrease of this zone and, consequently, in the joint strength decrease.

4 LABOR AND ENVIRONMENTAL PROTECTION

The main part of the study is conducted at laboratory of laser technology. Because of this all labor and environmental protection is related to laser radiation and its sources.

4.1 Safety precautions when working at ALTC "Sibir-1"

When operating laser equipment, there are a number of requirements for personnel. Persons at least 18 years old who have passed preliminary (upon admission) and periodic medical examination and instruction (preliminary and periodic) at the workplace are allowed to work on the automatic laser technological complex (ALTC) "Sibir-1".

Prior to being assigned to independent work, personnel are required to undergo preliminary training. Technological personnel must have an electrical safety admission group of at least II. Technological personnel are prohibited from taking part in commissioning work related to electrical safety or laser radiation.

4.2 Dangerous and harmful factors

During the operation of the laser system, the personnel may be affected by the following hazardous and harmful production factors:

- laser radiation (direct, scattered, reflected);
- high electrical voltage;
- hazardous gases and aerosols;
- heat;
- high noise from the installation.

According to [61,62] "Sibir-1" belongs to the installations of the 4th class according to the degree of hazard of the generated laser radiation. This means that the scattered radiation can damage the skin and create a fire hazard. To prevent injury from scattered radiation, the installation is equipped with a protective screen. The danger of high voltage is due to the fact that high power sources are used for this laser system. Hazardous gases and aerosols can be released during welding of

toxic materials such as lead or bismuth. The high noise is generated by the optical resonator during the operation of the installation.

According to this a workplace must contain the following:

- gloves (tarpaulin and cloth);
- cotton robe (overalls and suit);
- goggles against laser radiation, type 3H22-72C3CC22.
- dielectric personal protective gloves tested for voltages above 1000 V;
- noise-absorbing headphones;
- dielectric rugs;
- fire extinguishing equipment (sand, carbon dioxide fire extinguisher);
- medical kit.

To maintain fire safety, the workplace must be kept clean. There should be no flammable materials such as paper, wood, gasoline, etc. near the unit.

4.4 Regulated breaks

During work, a break is provided for rest and eating, the duration of which should be from 30 minutes to 2 hours. This break is not included in business hours. Also, when working in the cold season in the open air or in an unheated room, there are breaks included in the working hours. Also, such breaks can be established in cases when they are necessary to restore concentration [63].

4.4 Environmental protection

Unlike many welding methods, laser welding is environmentally friendly and safe (subject to safety precautions). During the process, inert gases (argon, helium) are used. Carbon dioxide is used as a laser medium, a high concentration of which leads to asphyxiation, but it is used in such a volume that its concentration cannot reach dangerous levels if leaked.

As mentioned above, hazardous gases and aerosols can be released when handling toxic materials. If such a process is required, safety measures are agreed with laboratory management.

4.5 Conclusions

Analyzing the above, we can conclude that the work at this enterprise is safe while observing safety precautions. The main part of the laboratory equipment, laser installations, poses a threat only in case of emergency situations, which can be avoided by observing the rules for working with this equipment.

5 ECONOMIC SECTION

This section presents the calculation of the cost of research work (R&D). To find it, we highlight the main stages of research:

- materials;
- materials preparation to the experiment;
- experiment;
- metallographic specimens preparation;
- tensile tests;
- recording and analysis of synchrotron radiation diffraction;
- scanning electron mycroscopy.

5.1 The procedure for calculating the cost of equipment operation

The costs at each stage of research and development consist of depreciation of equipment, material costs, salaries of employees involved in the work, electricity costs and other costs.

5.1.1 Depreciation of equipment

Equipment depreciation can be calculated using the formula:

$$A = \frac{P \cdot F_f}{F_n \cdot F_{sl}},$$

where P is the price of the equipment; F_f is the actual time of using the equipment, hour; F_n - nominal fund of equipment operation time, hour; F_{sl} - equipment service life, year.

5.1.2 Salary

Labor costs are made up of basic wages and pension contributions. Basic salary is calculated based on the salary:

$$L_o = T_c \cdot T_{pi},$$

where T_c is the tariff rate, rubles; T_{pi} is the actual running time.

Basic salary:

$$L_b = K \cdot L_0,$$

where K is the regional coefficient (1.2 for Novosibirsk)

Pension contributions:

$$L_{pens} = L_b \cdot 0{,}271$$

5.1.3 Electricity

Electricity costs can be found using the formula:

$$E = P \cdot N \cdot t_p,$$

where P is the cost of electricity, kW/hour; N - equipment power, kW; tp - equipment operation time, hours.

5.2 Calculation of the cost of research stages

Since many centers for collective use provide information on the cost of work, you can find the cost of each stage of R&D without calculating individual cost items. In this case, it is necessary to take into account the purchase price of the material (alloys) and its cutting.

5.2.1 Expenses for the purchase and cutting of materials

In total, 12 plates of titanium alloy VT-20 and aluminum alloy V-1461 with dimensions of 100x50x2 mm were used. The plates were laser cut. The utilization factor of the material is 0.86. The density of titanium alloy is 4400 kg / m3, the density of aluminum alloy is 2630 kg / m3. In terms of mass, the material consumption was 0.614 kg of VT-5 alloy and 0.377 kg of V-1461 alloy. The price of materials, taking into account the delivery of 1800 rubles / kg for VT-20 and 7000 rubles / kg for B-1461. Material costs amounted to RUB 3744.2.

Cutting costs are calculated based on the length of the cutting contour. The perimeter of one plate is 0.3 m. The total length of the contour is 7.2 m. The cost of cutting is about 50 rubles / m. The cost of cutting materials 360 rubles.

5.2.2 Experiment costs

The preparation of materials for the experiment and its implementation were carried out by the chief engineer of the enterprise. The preparation of the materials was carried out within 3 hours, the welding of the samples took 6 hours. The salary of the chief engineer is 250 rubles per hour. According to the calculations according to the formulas given above, the cost of wages amounted to 3431.7 rubles.

The operating cost of the installation is calculated according to the total length of the processed contour. The length of the contour on one sample is 0.1 m. The total length was 1.2 m. The price of 1 meter of a welded seam is approximately 100 rubles. The cost of the operation of the installation is 120 rubles.

5.2.3 Sample making

The samples were made using a cutting machine. In total, the production of all samples took 10 hours. The price of work on a cutting machine is 701.1 rubles / hour. The cost of making samples was 7011 rubles.

5.2.4 Mechanical tests

A total of 8 samples were tested for tensile strength. Tensile test price 2000r / sample. Costs amounted to 16000 rubles.

5.2.5 Metallographic research

For research, 3 thin sections were made. The cost of a full cycle of manufacturing 1 thin section is 4600 rubles. Costs amounted to 13,800 rubles.

Payment for studies on a scanning electron microscope for 1 shift (4 hours) is 8000 rubles. 1 shift was enough for research. Costs amounted to 8,000 rubles.

5.2.6 Phase analysis

The indexing of the diffraction patterns took about 45 hours. The salary of a laboratory assistant is 93 rubles/hour. Costs amounted to 4185 rubles.

5.3 Cost estimate

Cost estimate is presented in Table 9.

Table 9 — The cost estimate

№	Cost item name	Amount, rub.	The proportion of total costs, %
1	Purchase of materials	3744.2	6.6
2	Cutting materials	360	0.6
3	Salary	3431.7	6.4
4	Experiment	120	0.2
5	Sample making	7011	12.3
6	Tensile tests	16000	28.2
7	Metallographic specimens preparation	13800	24.3
8	Scanning electron microscopy	8000	14.1
9	Phase analysis	4185	7.3
10	TOTAL	56651.9	100

5.4 Conclusion

According to economic calculations, the cost of research work was 56651.9 rubles. including the costs of carrying out each of the stages, the experiment, the purchase and processing of materials and the salaries of the employees involved in this work.

CONCLUSION

Based on the purpose of the work, structural and phase studies and mechanical tests of dissimilar laser welded joints between pseudo-alpha titanium alloy VT-20 and aluminum alloy B1461 of the Al-Cu-Li system were carried out, obtained at various horizontal displacements of the focus of the laser beam towards the titanium alloy.

The research results showed that with insufficient displacement of the laser beam, the melts of the starting materials are mixed, and an extensive mixing region is formed, consisting of Ti_3Al, TiAl and β_2-Ti. in this case, the shift towards titanium led to an increase in the amount of aluminum in this interlayer.

With sufficient displacement, the melts of the materials do not contact, and the joint is formed by the welding-brazing mechanism. In this case, a thin (~2 μm) $TiAl_3$ interlayer is formed between the plate materials.

In all cases, the softening of the material of the aluminum alloy occurred in the zone of its melting due to the coagulation of the strengthening phases at the grain boundaries.

Mechanical tests have shown that beam displacement increases the strength of the joints (74 MPa for no offset, 107 MPa for 0.5 mm offset and 168 MPa for 1 mm offset).

The findings can be used to improve the properties of compounds obtained by contacting titanium and aluminum alloy melts. Since the phase composition of the mixing zone is similar to $\alpha_2 + \gamma$ TiAl intermetallic alloys, it is possible to use methods of increasing their plasticity for such welded joints – alloying with β-stabilizing components.

Since melting and subsequent crystallization do not allow obtaining the original structure of the aluminum alloy, even in offset welding, the strength of the joint is far from that of the original alloy. The structure can be restored by heat treatment close to that of the starting material, however, a strong composition contrast at the interface between the plates can lead to a thickening of the interlayer between them and a decrease in the strength of the joint.

References

1. **Lei, Z.** Microstructure and mechanical properties of welding–brazing of Ti/Al butt joints with laser melting deposition layer additive. / P. Li, X. Zhang, S. Wu et al. — // J. Manuf. Process. Elsevier Ltd, — 2019. — Vol. 38. — P. 411–421.
2. **Quazi, M.M.** Current research and development status of dissimilar materials laser welding of titanium and its alloys. / M. Ishak, M. A. Fazal, A. Arslan et al. — // Optics and Laser Technology. Elsevier Ltd, — 2020. — Vol. 126. — P. 106090.
3. **Liu, J.** Laser fusion-brazing of aluminum alloy to galvanized steel with pure Al filler powder. / S. Jiang, Y. Shi, Y. Kuang et al. — // Opt. Laser Technol. Elsevier, — 2015. — Vol. 66. — P. 1–8.
4. **Lazurenko, D. V.** Explosively welded multilayer Ti-Al composites: Structure and transformation during heat treatment. / I. A. Bataev, V. I. Mali, A. A. Bataev et al. — // Mater. Des. Elsevier B.V., — 2016. — Vol. 102. — P. 122–130.
5. **Chen, X.** Microstructure and tensile properties of Ti/Al dissimilar joint by laser welding-brazing at subatmospheric pressure. / Z. Lei, Y. Chen, Y. Han et al. — // J. Manuf. Process. Elsevier Ltd, — 2020. — Vol. 56. — P. 19–27.
6. **Zhou, X.** The Study on Mechanical Strength of Titanium-Aluminum Dissimilar Butt Joints by Laser Welding-Brazing Process. / J. Duan, F. Zhang, S. Zhong. — // Materials (Basel). — 2019. — Vol. 12, № 5. — P. 712.
7. **Tomashchuk, I.** Aluminum to titanium laser welding-brazing in V-shaped groove. / P. Sallamand, A. Méasson, E. Cicala et al. — // J. Mater. Process. Technol. Elsevier, — 2017. — Vol. 245. — P. 24–36.
8. **Chen, X.** Effect of Laser Beam Oscillation on Laser Welding–Brazing of Ti/Al Dissimilar Metals. / Z. Lei, Y. Chen, Y. Han et al. — // Materials (Basel). MDPI AG, — 2019. — Vol. 12, № 24. — P. 4165.
9. **Chen, Y.** Influence of interfacial reaction layer morphologies on crack initiation and propagation in Ti/Al joint by laser welding-brazing. / S. Chen,

L. Li. — // Mater. Des. Elsevier Ltd, — 2010. — Vol. 31, № 1. — P. 227–233.

10. **Li, L.** Tungsten inert gas welding of dissimilar metals aluminum to titanium with aluminum based wire. / B. Zhao, X. Wu. — // Mater. Res. Express. IOP Publishing, — 2019. — Vol. 6, № 5. — P. 056561.
11. **Wei, S.** Cold Arc MIG Welding of Titanium Ti6Al4V to Aluminum 5A05Al Using Al–Mg5 Filler. / W. Rao, Z. Li, Y. Zhang. — // Met. Mater. Int. Korean Institute of Metals and Materials, — 2019.
12. **Wei, S.** Use of welding-brazing technology on microstructural development of titanium/aluminum dissimilar joints. / Y. Li, J. Wang, K. Liu. — // Mater. Manuf. Process. — 2014. — Vol. 29, № 8. — P. 961–968.
13. **Chen, X.** Ultrasonic-assisted brazing of Al-Ti dissimilar alloy by a filler metal with a large semi-solid temperature range. / R. Xie, Z. Lai, L. Liu et al. — // Mater. Des. Elsevier B.V., — 2016. — Vol. 95. — P. 296–305.
14. **Chang, S.Y.** Brazing of 6061 aluminum alloy/Ti-6Al-4V using Al-Si-Cu-Ge filler metals. / L. C. Tsao, Y. H. Lei, S. M. Mao et al. — // J. Mater. Process. Technol. Elsevier B.V., — 2012. — Vol. 212, № 1. — P. 8–14.
15. **Wei, Y.** Formation process of the bonding joint in Ti/Al diffusion bonding. / W. Aiping, Z. Guisheng, R. Jialie. — // Mater. Sci. Eng. A. — 2008. — Vol. 480, № 1–2. — P. 456–463.
16. **Choi, J.-W.W.** Dissimilar friction stir welding of pure Ti and pure Al. / H. Liu, H. Fujii. — // Mater. Sci. Eng. A. Elsevier Ltd, — 2018. — Vol. 730. — P. 168–176.
17. **Kar, A.** Effect of niobium interlayer in dissimilar friction stir welding of aluminum to titanium. / S. K. Choudhury, S. Suwas, S. V. Kailas. — // Mater. Charact. Elsevier, — 2018. — Vol. 145, № September. — P. 402–412.
18. **Kar, A.** Effect of Mechanical Mixing in Dissimilar Friction Stir Welding of Aluminum to Titanium with Zinc Interlayer. / S. V. Kailas, S. Suwas. — // Trans. Indian Inst. Met. Springer India, — 2019. — Vol. 72, № 6. — P. 1533–1536.
19. **Wu, A.** Interface and properties of the friction stir welded joints of titanium

alloy Ti6Al4V with aluminum alloy 6061. / Z. Song, K. Nakata, J. Liao et al. — // Mater. Des. Elsevier Ltd, — 2015. — Vol. 71. — P. 85–92.

20. **Mahmood, Y.** Experimental and Numerical Study on Microstructure and Mechanical Properties of Ti-6Al-4V/Al-1060 Explosive Welding. / K. Dai, P. Chen, Q. Zhou et al. — // Metals (Basel). — 2019. — Vol. 9, № 11. — P. 1189.
21. **Casalino, G.** Off-Set and Focus Effects on Grade 5 Titanium to 6061 Aluminum Alloy Fiber Laser Weld. / S. D'Ostuni, P. Guglielmi, P. Leo et al. — // Materials (Basel). — 2018. — Vol. 11, № 11. — P. 2337.
22. **Song, Z.** Interfacial microstructure and mechanical property of Ti6Al4V/A6061 dissimilar joint by direct laser brazing without filler metal and groove. / K. Nakata, A. Wu, J. Liao. — // Mater. Sci. Eng. A. Elsevier, — 2013. — Vol. 560. — P. 111–120.
23. **Leo, P.** Low temperature heat treatments of AA5754-Ti6Al4V dissimilar laser welds: Microstructure evolution and mechanical properties. / S. D'Ostuni, G. Casalino. — // Opt. Laser Technol. — 2018. — Vol. 100. — P. 109–118.
24. **Guo, S.** Microstructure and mechanical characterization of re-melted Ti-6Al-4V and Al-Mg-Si alloys butt weld. / Y. Peng, C. Cui, Q. Gao et al. — // Vacuum. Elsevier, — 2018. — Vol. 154, № April. — P. 58–67.
25. **Malikov, A.** Effect of the aluminum alloy composition (Al-Cu-Li or Al-Mg-Li) on structure and mechanical properties of dissimilar laser welds with the Ti-Al-V alloy. / I. Vitoshkin, A. Orishich, A. Filippov et al. — // Opt. Laser Technol. Elsevier Ltd, — 2020. — Vol. 126. — P. 106135.
26. **Malikov, A.** Microstructure and mechanical properties of laser welded joints of Al-Cu-Li and Ti-Al-V alloys. / I. Vitoshkin, A. Orishich, A. Filippov et al. — // J. Manuf. Process. Elsevier Ltd, — 2020. — Vol. 53. — P. 201–212.
27. **Nikulina, A.A.** Special Features of the Structure of Laser-Welded Joints of Dissimilar Alloys Based on Titanium and Aluminum. / A. I. Smirnov, G. A. Turichin, O. G. Klimova-Korsmik et al. — // Met. Sci. Heat Treat. — 2017. — Vol. 59, № 7–8. — P. 534–539.

28. **Casalino, G.** Modeling and experimental analysis of fiber laser offset welding of Al-Ti butt joints. / M. Mortello. — // Int. J. Adv. Manuf. Technol. — 2016. — Vol. 83, № 1–4. — P. 89–98.
29. **Tushinsky, L.I.** Structural theory of constructional strength of materials [In Russian]. Novosibirsk : 2004. — 410 p.
30. **Patent № CN102229018A** Argon arc welding method suitable for self connection of TiAl-based alloy material declared: 2011 / W. Liu, H. Xiong, S. Guo et al. — 6 p.
31. **Patent № US4486647A** Method of welding aluminum to titanium and a welded joint so produced declared: 1981 / O. Kuusinen, M. Rantanen, O. Rintanen et al. — 7 p.
32. **Patent № CN102554456A** Diffusion welding method for titanium-aluminum based alloy and titanium alloy added amorphous interlayer declared: 2012 / Z. Xue, Y. Huang, Y. Wang et al. — 6 p.
33. **Patent № CN102896406A** TIG welding method of titanium alloy and pure aluminum plates declared: 2012 / Y. Xia. — 7 p.
34. **Patent № CN102229019B** Argon arc welding method suitable for TiAl-based alloy material and titanium alloy declared: 2011 / H. Xiong, W. Liu, S. Guo et al. — 6 p.
35. **Patent № US5844198A** Technique for laser welding dissimilar metals declared: 1995 / S.M. Jones, A.A. Campbell, J.L. Pennala. — 10 p.
36. **Patent № CN106735948A** A kind of method for laser welding and its device of copper aluminium dissimilar metal declared: 2017 / W. Shi, J. Huang, Y. Xie et al. — 8 p.
37. **Patent № CN102764934A** Aluminum steel dissimilar metal laser welding-brazing welding method and filled powder declared: 2012 / D. Fan, K. Jiang, S. Yu et al. — 12 p.
38. **Patent № US9174298B2** Dissimilar metal joining method for magnesium alloy and steel declared: 2009 / M. Kasukawa, S. Nakagawa, K. Miyamoto. — 10 p.

39. **Patent № US20050230371A1** Laser roll joining method for dissimilar metals and laser roll joining apparatus declared: 2003 / M. Kutsuna, A. Tsuboi, M. Rathod. — 24 p.
40. **Tomashchuk, I.** Direct keyhole laser welding of aluminum alloy AA5754 to titanium alloy Ti6Al4V. / P. Sallamand, E. Cicala, P. Peyre et al. — // J. Mater. Process. Technol. Elsevier B.V., — 2015. — Vol. 217. — P. 96–104.
41. **Zhang, C.** Interfacial Segregation of Alloying Elements During Dissimilar Ultrasonic Welding of AA6111 Aluminum and Ti6Al4V Titanium. / J. D. Robson, S. J. Haigh, P. B. Prangnell. — // Metall. Mater. Trans. A Phys. Metall. Mater. Sci. Springer Boston, — 2019. — Vol. 50, № 11. — P. 5143–5152.
42. **Ilyin, A.A.** Titanium alloys. Composition, structure, properties [In Russian]. / B. A. Kolachev, I. C. Polkin. — Москва : ВИЛС-МАТИ. 2009. — 520 p.
43. **Khokhlatova, L.B.** Aluminum-lithium alloys for aircraft manufacturing. / N. I. Kolobnev, M. S. Oglodkov, E. D. Mikhaylov. — // Metallurg. — 2012. — Vol. 5. — P. 31–35.
44. **GOST 19807-91**. Wrought titanium and titanium alloys. Grades [In Russian]. — Intr. 1992-07-01. — M.: Publishing house of standards, 1992. — Text: direct.
45. **Malikov, A.** Manufacturing of high-strength laser welded joints of an industrial aluminum alloy of system Al-Cu-Li by means of post heat treatment. / A. Orishich, A. Golyshev, E. Karpov. — // J. Manuf. Process. Elsevier, — 2019. — Vol. 41. — P. 101–110.
46. **Malikov, A.G.** Control of the mechanical properties and microstructure of laser welded joints of the aluminum alloy V-1461 after heat treatment. / A. M. Orishich, E. V Karpov, I. E. Vitoshkin. — // Mater. Phys. Mech. — 2020. — Vol. 43, № 1.
47. **Massalski, T.B.** Binary Alloy Phase Diagrams-Second edition. Ohio : ASM International. 1990. — 3589 p.
48. **Kad, B.K.** Effect of solidification velocity and nitrogen contamination on α

formation in a Ti-54at%Al melt. / B. F. Oliver. — // Scr. Metall. Mater. Pergamon, — 1992. — Vol. 26, № 12. — P. 1809–1812.

49. **Kattner, U.R.** Thermodynamic assessment and calculation of the Ti-Al system. / J.-C. C. Lin, Y. A. Chang. — // Metall. Trans. A, Phys. Metall. Mater. Sci. Springer, — 1992. — Vol. 23 A, № 8. — P. 2081–2090.

50. **Braun, J.** Phase Equilibria Investigations on the Aluminum-Rich Part of the Binary System Ti-Al. / M. Ellner. — // Metall. Mater. Trans. A Phys. Metall. Mater. Sci. — 2001. — Vol. 32A. — P. 1037–1047.

51. **Audier, M.** Structural relationships in intermetallic compounds of the Al-Li-(Cu, Mg, Zn) system. / C. Janot, M. De Boissieu, B. Dubost. — // Philos. Mag. B Phys. Condens. Matter; Stat. Mech. Electron. Opt. Magn. Prop. Taylor & Francis Group , — 1989. — Vol. 60, № 4. — P. 437–466.

52. **Chen, H.S.** Thermodynamic properties and phase diagram of icosahedral AlxLi3Cu. / A. R. Kortan, J. M. Parsey. — // Phys. Rev. B. American Physical Society, — 1987. — Vol. 36, № 14. — P. 7681–7684.

53. **Leblanc, M.** Crystalline phases related to the icosahedral Al-Li-Cu phase. A single crystal X-ray diffraction study of the tetragonal τ-Al56(Cu, Zn)11Li33 phase. / A. Le Bail, M. Audier. — // Phys. B Phys. Condens. Matter. North-Holland, — 1991. — Vol. 173, № 3. — P. 329–355.

54. **Dubost, B.** Constitution and Thermodynamics of Quasicrystalline and Crystalline Al-Cu-Li Alloys. / C. Colinet, I. Ansara. — // ILL/CODEST Work. Quasicrystals. — 1988. — Vol. 22. — P. 39–52.

55. **Loretto, M.H.** Microstructural studies on some ordered Ti-based alloys. / D. Hu, Y. G. Li. — // Intermetallics. Elsevier Science Ltd, — 2000. — Vol. 8, № 9–11. — P. 1243–1249.

56. **Imayev, V.** Microstructure and mechanical properties of low and heavy alloyed γ-TiAl + α 2-Ti 3Al based alloys subjected to different treatments. / T. Oleneva, R. Imayev, H. J. Christ et al. — // Intermetallics. Elsevier, — 2012. — Vol. 26. — P. 91–97.

57. **Lacom, W.** Low temperature decomposition in binary AlLi alloys. / //

Zeitschrift fuer Met. Res. Adv. Tech. — 1990. — Vol. 81, № 9. — P. 663–667.

58. **Yoshi-Yama, T.** Al3Li Superlattice in Al-4.5wt.% Li Alloy. / K. Hasebe, M. H. Mannam. — // J. Phys. Soc. Japan. THE PHYSICAL SOCIETY OF JAPAN, — 1968. — Vol. 25, № 3. — P. 908.
59. **Zinkevich, M.** Al-Cu-Li Ternary Phase Diagram Evaluation · Phase diagrams, crystallographic and thermodynamic data: Datasheet from MSI Eureka in SpringerMaterials (https://materials.springer.com/msi/docs/sm_msi_r_10_015854_02). / T. Velikanova, M. Turchanin, Z. Du et al. — / ed. Effenberg G. MSI Materials Science International Services GmbH.
60. **Minonishi, Y.** Plastic deformation of single crystals of Ti3Al with D019 structure. / // Philos. Mag. A Phys. Condens. Matter, Struct. Defects Mech. Prop. Taylor & Francis Group, — 1991. — Vol. 63, № 5. — P. 1085–1093.
61. **GOST R 50723-94**. Laser safety. General safety requirements for the development and operation of laser products [In Russian]. — Intr. 1996-01-01. — M.: Publishing house of standards, 1995. — Text: direct.
62. **SanRaN № 5804-91**. Sanitary norms and rules for the device and operation of lasers [In Russian]. — Intr. 1991-31-06. — Text: direct.
63. **Russian Federation**. Labor Code: Official text [In Russian].

Appendix A

Patents list

№	Patent mark	Inventor	Year	Patent title
1	CN102229018A	Liu Wenhui Xiong Huaping Guo Shaoqing Zhang Xuejun Zhou Biao Li Neng	2011	Argon arc welding method suitable for self connection of TiAl-based alloy material
2	US4486647A	Osmo Kuusinen Mikko Rantanen Olavi Rintanen Reijo Pajunen Pekka Oittinen Kalevi Valtanen	1981	Method of welding aluminum to titanium and a welded joint so produced
3	CN102554456A	Xue Zhiyong Huang Yuanxun Wang Yongtian Chen Yufeng Xu Gang Zhang Xiaoyan	2012	Diffusion welding method for titanium-aluminum based alloy and titanium alloy added amorphous interlayer
4	CN102896406A	Xia Yu	2012	TIG welding method of titanium alloy and pure aluminum plates
5	CN102229019B	Xiong Huaping Liu Wenhui Guo Shaoqing Zhang Xuejun Zhou Biao Li Neng	2011	Argon arc welding method suitable for TiAl-based alloy material and titanium alloy
6	US5844198A	Stephen M. Jones Arthur A. Campbell Jeffrey L. Pennala	1996	Technique for laser welding dissimilar metals
7	CN106735948A	Shi Wenqing Huang Jiang Xie Yuping An Fenju Li Sidong Li Yongqiang Wu Zhanxia	2017	A kind of method for laser welding and its device of copper aluminium dissimilar metal
8	CN102764934A	Fan Ding Jiang Kai Yu Shurong Huang Jiankang	2012	Aluminum steel dissimilar metal laser welding-brazing welding method and filled powder
9	US9174298B2	Minoru Kasukawa Shigeyuki Nakagawa Kenji Miyamoto	2009	Dissimilar metal joining method for magnesium alloy and steel
10	US20050230371A1	Muneharu Kutsuna Akihiko Tsuboi Manoj Rathod	2003	Laser roll joining method for dissimilar metals and laser roll joining apparatus